Article

TRANSPARENT PROCESS

THE EMBO JOURNAL

The E3 ubiquitin ligase APC/C^{Cdh1} degrades MCPH1 after MCPH1-βTrCP2-Cdc25A-mediated mitotic entry to ensure neurogenesis

Xiaoqian Liu[1], Wen Zong[1], Tangliang Li[1,2], Yujun Wang[3], Xingzhi Xu[4,5], Zhong-Wei Zhou[1,*] & Zhao-Qi Wang[1,6,**]

Abstract

Mutations of microcephalin (MCPH1) can cause the neurodevelopmental disorder primary microcephaly type 1. We previously showed that MCPH1 deletion in neural stem cells results in early mitotic entry that distracts cell division mode, leading to exhaustion of the progenitor pool. Here, we show that MCPH1 interacts with and promotes the E3 ligase βTrCP2 to degrade Cdc25A independent of DNA damage. Overexpression of βTrCP2 or the knockdown of Cdc25A remedies the high mitotic index and rescues the premature differentiation of *Mcph1*-deficient neuroprogenitors *in vivo*. MCPH1 itself is degraded by APC/C^{Cdh1}, but not APC/C^{Cdc20}, in late mitosis and G1 phase. Forced MCPH1 expression causes cell death, underlining the importance of MCPH1 turnover after mitosis. Ectopic expression of Cdh1 leads to premature differentiation of neuroprogenitors, mimicking differentiation defects of *Mcph1*-knockout neuroprogenitors. The homeostasis of MCPH1 in association with the ubiquitin-proteasome system ensures mitotic entry independent of cell cycle checkpoint. This study provides a mechanistic understanding of how MCPH1 controls neural stem cell fate and brain development.

Keywords Cdh1; cell cycle progression; MCPH1; neurogenesis; βTrCP2
Subject Categories Cell Cycle; Neuroscience
DOI 10.15252/embj.201694443 | Received 29 March 2016 | Revised 3 October 2017 | Accepted 4 October 2017 | Published online 17 November 2017
The EMBO Journal (2017) 36: 3666–3681

Introduction

Human primary microcephaly (MCPH, OMIM251200) is an autosomal recessive neurodevelopmental disorder, which is characterized by a marked reduction in brain size with a normal architecture and non-progressive mental retardation (Roberts *et al*, 2002). So far, 12 gene loci have been identified to be responsible for MCPH (reviewed by Kaindl, 2014), 10 of which encode proteins that are associated with centrosome or mitotic spindle poles, which function in controlling cell division (Hussain *et al*, 2013; Chavali *et al*, 2014; Mirzaa *et al*, 2014).

Microcephalin (MCPH1), encoded by *MCPH1*, is a scaffold protein and is responsible for type I MCPH. MCPH1 contains three breast cancer carboxyl terminal (BRCT) domains, one in the N-terminus and the other two are tandem arranged in the C-terminus (Yu *et al*, 2003; Lin *et al*, 2010). The N-terminal BRCT domain of MCPH1 mediates its centrosome localization after DNA damage and is required for binding to the SWI/SNF complex to regulate DNA repair (Peng *et al*, 2009). The two C-terminal BRCT domains bind to γ-H2AX and are necessary for the recruitment of BRCA2/RAD51 to the damage sites for the execution of homologous recombination (HR) repair (Jeffers *et al*, 2008; Lin *et al*, 2010). Additionally, the C-terminal BRCTs interact with E2F1, which promotes the transcription of DNA repair genes, such as BRCA1 and CHK1 (Yang *et al*, 2008). MCPH1 also interacts, through its central region, with condensin II, which is thought to prevent premature chromosome condensation (PCC), a characteristic of MCPH1 cells (Trimborn *et al*, 2006).

Human MCPH1 patient cells show a defective G2-M checkpoint, which is characterized by an impaired degradation of Cdc25A and hypo-phosphorylated Cdk1 due to a defective ATR-CHK1 activation (Xu *et al*, 2004; Lin *et al*, 2005; Alderton *et al*, 2006; Rai *et al*, 2006; Wood *et al*, 2008). We have generated a mouse model for MCPH1 with a null mutation of *Mcph1 (Mcph1-del)*. These mutant mice exhibit microcephaly, which is characterized by a reduced thickness of the neocortex at birth, mimicking human MCPH1 patients (Gruber *et al*, 2011; Zhou *et al*, 2013). The genetic ablation of *Mcph1* causes a premature differentiation of neuroprogenitors, thereby affecting spindle alignment and shifting the neuroprogenitor division mode from symmetric to asymmetric (Gruber *et al*, 2011). The

1 Leibniz Institute on Aging – Fritz Lipmann Institute (FLI), Jena, Germany
2 Institute of Aging Research, School of Medicine, Hangzhou Normal University, Hangzhou, China
3 Division of Biology, City of Hope National Medical Center/Beckman Research Institute, Duarte, CA, USA
4 Beijing Key Laboratory of DNA Damage Response, College of Life Sciences, Capital Normal University, Beijing, China
5 Guangdong Key Laboratory for Genome Stability & Disease Prevention, Shenzhen University School of Medicine, Shenzhen, Guangdong, China
6 Faculty of Biology and Pharmacy, Friedrich-Schiller University of Jena, Jena, Germany
*Corresponding author. Tel: +49 3641 656420; E-mail: zhongwei.zhou@fli-leibniz.de
**Corresponding author. Tel: +49 3641 656415; Fax: +49 3641 656413; E-mail: zhao-qi.wang@leibniz-fli.de

© 2017 The Authors

hypo-phosphorylation of Cdk1 is found in *Mcph1*-del neuroprogenitors and correlates with a premature mitotic entry. The DNA damage response (DDR) function of MCPH1 cannot explain in full its physiological role in neurogenesis (Gruber *et al*, 2011; Zhou *et al*, 2013). Thus, the function of MCPH1 in regulating the G2-M checkpoint is believed to be responsible for the microcephaly phenotype.

Two major ubiquitin E3 ligase complexes are implicated in cell cycle progression: the Skp1-Cul1-F-box (SCF) complex and the anaphase-promoting complex/cyclosome (APC/C) complex (Vodermaier, 2004). The β-transducin repeat-containing protein (βTrCP) is one of the F-box proteins that are responsible for the recruitment of specific substrates into the SCF complex (Suzuki *et al*, 1999). In mammals, there are two paralogs of βTrCP, namely βTrCP1 and βTrCP2 (also known as BTRC/FBXW1 and FBXW11, respectively; Suzuki *et al*, 1999). Both βTrCPs can degrade Cdc25A in response to DNA damage (Busino *et al*, 2003), which requires primed phosphorylation on Ser76 by CHK1 (Busino *et al*, 2003; Jin *et al*, 2003). APC/C is another ubiquitin E3 ligase complex, which has two activators, Cdc20 and Cdh1. While APC/C^{Cdc20} plays a role in the early phase of mitosis and in metaphase/anaphase transition, APC/C^{Cdh1} is activated in the mitotic exit and the early G1 phase to ensure G1 phase progression and to prevent S-phase entry (van Leuken *et al*, 2008; Meghini *et al*, 2016). It is also shown that a deletion of Cdh1 delays neurogenesis (van Leuken *et al*, 2008; Delgado-Esteban *et al*, 2013).

In this report, we discover that MCPH1 directly regulates the Cdc25A stability through an interaction with and the promotion of the dimerization of βTrCP2 to ensure mitotic entry, but MCPH1 itself is degraded in late M phase and mainly in G1 phase in order to prevent cell death. The concerted action of Cdh1-MCPH1-βTrCP2-Cdc25A by the ubiquitin-proteasome system (UPS) decides neuroprogenitor fate and thus, provides a key mechanism for brain development.

Results

The identification of the MCPH1 interacting partners by a yeast two-hybrid (Y2H) screen

Studies using MCPH1 mutant cellular and mouse models have shown an alteration of the G2-M transition and neuroprogenitor differentiation process after the MCPH1 inactivation (Xu *et al*, 2004; Lin *et al*, 2005; Alderton *et al*, 2006; Rai *et al*, 2006; Wood *et al*, 2008). Since MCPH1 is a scaffold protein, we hypothesized that its role in neuro-stem cell fate determination is thus likely through its effectors or partners. To search for these interaction partners, we carried out a yeast two-hybrid (Y2H) screen to identify novel MCPH1 partners by using a cDNA fragment encoding a polypeptide of the 96–612AA of human MCPH1 without all three BRCT domains as the bait. This would greatly reduce the number of MCPH1 interactors that are functionally associated with DDR. A total of 99 LacZ-positive colonies were obtained from three independent screens. Seventy-seven coding sequences from 66 genes with known functions were confirmed by sequencing (Table EV1). Among these coding genes, we focused on *FBXW11* that encodes βTrCP2, which is a WD40 domain-containing F-box protein responsible for substrate binding in the SCF ubiquitin E3 ligase complex.

MCPH1 interacts with βTrCP2 *in vivo*

To verify the interaction between MCPH1 and βTrCP2, HA-tagged MCPH1 (HA-MCPH1) and FLAG-tagged βTrCP2 (FLAG-βTrCP2) or βTrCP1 (FLAG-βTrCP1) were co-transfected into 293T cells. Co-immunoprecipitation (Co-IP) assays revealed that HA-MCPH1 interacted strongly and specifically with FLAG-βTrCP2, but negligibly with FLAG-βTrCP1 (Fig 1A). This interaction was further confirmed by Co-IP showing that ectopic expressed FLAG-βTrCP2 (Fig 1B) or endogenous βTrCP2 (Fig 1C) was present in the endogenous MCPH1 immunocomplex (Fig 1B and C). To determine whether MCPH1 also binds to other WD40 domain-containing F-box proteins or to other components of the SCF complex, we co-transfected HA-MCPH1 with FLAG-tagged FBW7, Skp2, or Skp1 into 293T cells and found that MCPH1 bound mainly to βTrCP2 (Fig 1D). Because MCPH1 is involved in DDR (Xu *et al*, 2004; Lin *et al*, 2010), we next asked whether the interaction between MCPH1 and βTrCP2 is DDR-dependent. Co-IP assays were carried out at the different time point after treating cells with a low does (2 Gy) and a high does (10 Gy) of ionizing radiation (IR). A low dose (2 Gy) of IR did not change the MCPH1 level till 24 h after irradiation (Fig EV1A). However, 10 Gy IR reduced the MCPH1 protein level, which correlates well with DDR, judged by the super-shifted Chk2, which is an indication of phosph-Chk2 (Fig 1E). However, neither dose of IR disrupts the interaction between MCPH1 and βTrCP2 in the Co-IP (Figs 1E and EV1A). These data suggest that MCPH1 interacts with βTrCP2 *in vivo* under unperturbed conditions and also upon DNA damage.

We next mapped the interacting regions among MCPH1 and βTrCP2. To this end, different truncations of MCPH1 and βTrCP2 were prepared (Fig 1F and G). A Co-IP analysis showed that βTrCP2 bound to wild-type MCPH1 as well as mutant MCPH1 with a deletion of individual or all BRCT domains (Fig 1F). Thus, BRCT domains are not necessary for the interaction, which is consistent with the original Y2H data. The interaction most likely takes place in the middle part of MCPH1. We then investigated which domain of βTrCP2 is responsible for the interaction with MCPH1. An IP assay revealed that the interaction between MCPH1 and βTrCP2 was not affected by truncating βTrCP2 neither in the N-terminus (ΔN), which includes the D domain that is required for dimer formation, nor in the F-box domain (ΔF) that binds to Skp1, although these truncations showed less affinity to MCPH1 compared to full-length βTrCP2 (Fig 1G). Of note, the βTrCP2 truncation without a C-terminal WD40-containing domain, which is required for substrate binding, completely lost the ability to pull down MCPH1 (Fig 1G), suggesting that MCPH1 may be a substrate of βTrCP2 or may antagonize other substrates of βTrCP2.

MCPH1 is not a substrate for βTrCP2, but stimulates its activity to degrade Cdc25A

Next, we examined whether $SCF^{βTrCP2}$ degrades MCPH1. The MCPH1 level was not affected when it was co-expressed with βTrCP2 in 293T cells (Figs 1A, B, D and F, and EV1B). Moreover, knockdown of βTrCP2 (Fig EV1C) did not increase the endogenous MCPH1 level (Fig EV1D). Since 10 Gy IR reduced endogenous MCPH1 as well as βTrCP2 (see Fig 1E), we wondered whether MCPH1 degradation was mediated by βTrCP2 in DDR. To test this, cells ectopically expressing MCPH1 and βTrCP2 were exposed to 10 Gy of IR. No

© 2017 The Authors

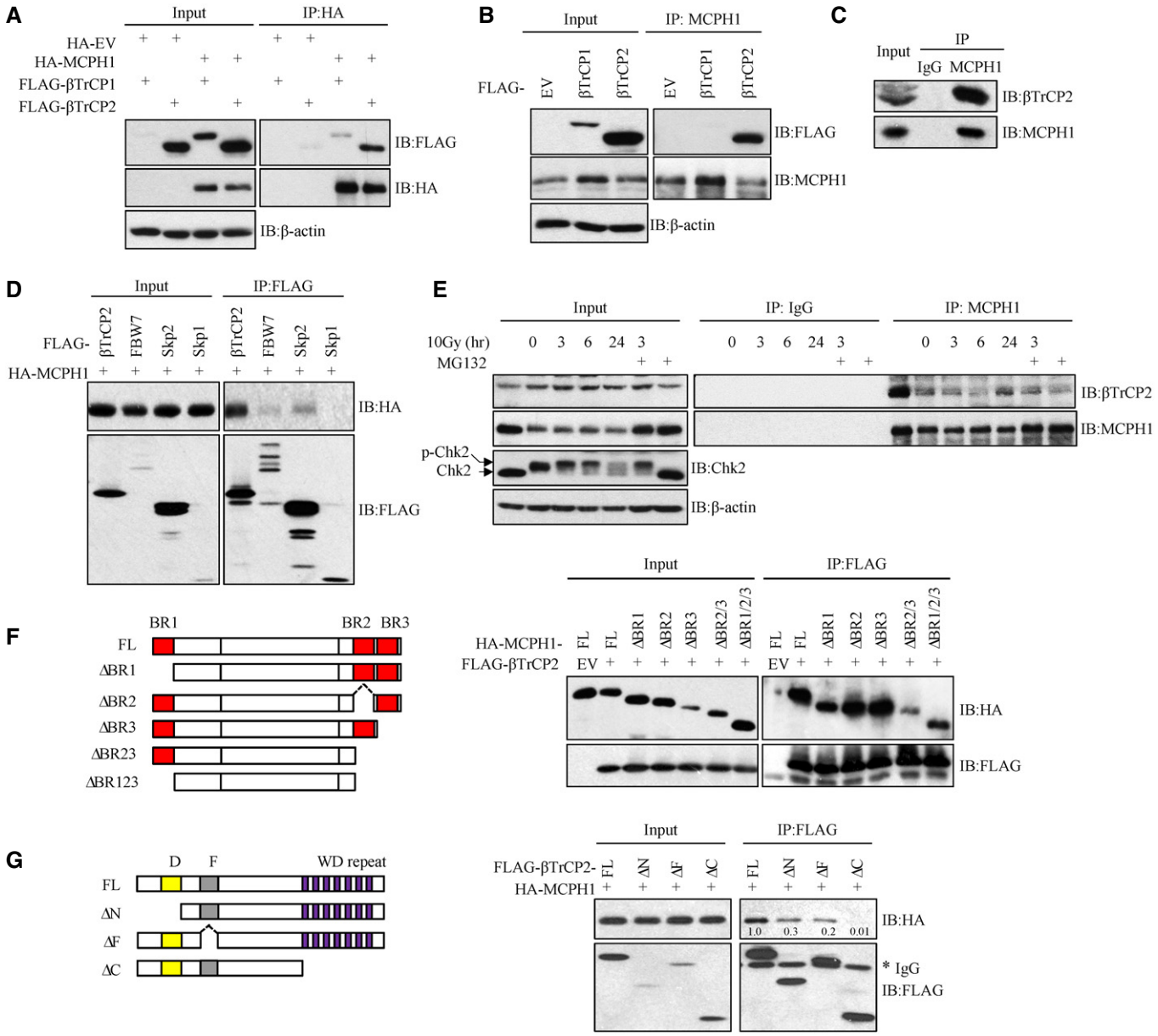

Figure 1. Interaction of MCPH1 with βTrCP2.

A HA-MCPH1 interacted with FLAG-βTrCP2. HA-MCPH1 was co-transfected with FLAG-βTrCP1 or FLAG-βTrCP2 into 293T cells. Immunoprecipitation (IP) was performed using anti-FLAG antibody, and immunoblotting (IB) was performed using anti-FLAG or anti-HA antibody. The experiment was repeated twice.

B Co-IP assay of endogenous MCPH1 was performed using an anti-MCPH1 antibody in 293T cells after transfection with FLAG-βTrCP1 or FLAG-βTrCP2. The experiment was repeated twice.

C Endogenous MCPH1 interacts with βTrCP2 in Neuro2A cells. IP was performed using an anti-MCPH1 antibody, and IB was performed using anti-MCPH1 or anti-βTrCP2 antibody.

D HA-MCPH1 was co-transfected with FLAG-tagged indicated F-box protein constructs. IP and IB were performed using anti-HA or FLAG antibody as indicated.

E Neuro2A cells were treated with 10 Gy ionizing radiation (IR) with or without the proteasome inhibitor MG132 and harvested at the indicated time after IR. Endogenous Co-IP was performed using an anti-MCPH1 antibody, and IB was performed using an anti-MCPH1 or anti-βTrCP2 antibody. The experiment was repeated twice.

F Left panel: Schematic diagram of full-length and deletion mutants of MCPH1. Red boxes represent the BRCT domain. FL: 1–835aa, ΔBR1: 94–835aa, ΔBR2: Δ671–730aa, ΔBR3: 1–730aa, ΔBR2-3: 1–670aa. Right panel: HA-tagged full-length and deletion mutants of MCPH1 were co-transfected with FLAG-βTrCP2. IP and IB were performed using the anti-FLAG or anti-HA antibody. The experiment was repeated twice.

G Left panel: Schematic diagram of βTrCP2 full-length and a series of deletion mutants. The yellow box represents the D domain, the gray box represents the F-box domain, and purple box represents the WD domain. FL: 1–529aa, ΔN: 121–529aa, ΔF: Δ129–167aa, ΔC: 1–237aa. Right panel: HA-MCPH1 was co-transfected with indicated βTrCP2 deletion mutants. IP and IB were performed using anti-FLAG or anti-HA antibody. Input in each panel is 10% of total cell lysates. The FLAG-EV or HA-EV blots are not shown because their size is too small to be included. The number under each sample is a ratio to the FL sample after normalization to Input of the displayed blots. Asterisk marks the IgG band.

 © 2017 The Authors

obvious reduction in the level of MCPH1 found in βTrCP2 expressing cells, compared to EV-transfected samples after 10 Gy IR treatments (Fig EV1E). Thus, MCPH1 is most likely not a substrate of βTrCP2 under either unperturbed or DNA damage conditions. To further address the meaning of the interaction between MCPH1 and βTrCP2, we tested whether this interaction modulates the βTrCP2 activity by examining the status of $SCF^{\beta TrCP2}$ substrates Cdc25B and Cdc25A (Busino *et al*, 2003; Thomas *et al*, 2010; Young & Pagano, 2010). While we did not observe an obvious reduction of Cdc25B when co-transfected with βTrCP2 (Fig EV1F and G, lanes 3 and 8), an overexpression of βTrCP2 reduced the Cdc25A level to a level similar to shCdc25A (Fig EV1G, lanes 3 and 4). Interestingly, when we knocked down MCPH1 by shRNA, we detected a higher level of endogenous as well as of ectopically expressed Cdc25A compared to shLuc controls (Figs 2A and B, and EV1G), suggesting that Cdc25A is a target of MCPH1-βTrCP2 interaction.

To further confirm these findings, HA-Cdc25A and FLAG-βTrCP2 were co-transfected with or without the shMCPH1 expression vectors into 293T cells. The HA-Cdc25A levels were greatly reduced in the cells co-expressing FLAG-βTrCP2, as compared to the FLAG-EV (empty vector) control (Fig 2B, Input, lanes 1 and 2). The knockdown of MCPH1 by shRNA led to a high level of Cdc25A (Fig 2B, Input, lanes 1 and 4) and strongly suppressed βTrCP2-mediated Cdc25A degradation (Fig 2B, Input, lanes 2 and 5). In both cases, Cdc25A was further stabilized by a treatment with a proteasome inhibitor MG132 (Fig 2B, Input, lanes 2 and 3, lanes 5 and 6). Reversely, an overexpression of MCPH1 decreased the Cdc25A level (Fig 2C, lane 4), which was further enhanced by an ectopic expression of βTrCP2 (Fig 2C, lane 5). Next, we measured the stability and kinetics of Cdc25A in shMCPH1-transfected cells using cycloheximide (CHX), a protein synthesis inhibitor. While Cdc25A was gradually degraded during the time course of the CHX treatment in control shLuc-transfected 293T cells, it stayed at a high level in shMCPH1 cells (Figs 2D, and EV2A and B), suggesting that the Cdc25A degradation is dependent on MCPH1. To further identify during which cell cycle phase MCPH1-mediated degradation of Cdc25A occurs, we measured the stability and kinetics of endogenous Cdc25A in S (1 and 4 h) and G2 (6 h) phases after releasing from double-thymidine (T-T) block which synchronized cells in the early S-phase, together with the CHX treatment (Fig EV2C and D). The increased stability of Cdc25A after MCPH1 deletion was mainly found in G2 phase (Fig EV2C). At each time point, we also analyzed Cdc25A mRNA and found that Cdc25 mRNA was relatively lower compared to controls (Fig EV2E), ruling out that the increased Cdc25A protein in shMCPH1 cells is due to the Cdc25A transcription. In addition, the increased stability of Cdc25A in G2 phase was also observed after βTrCP2 knockdown (Fig EV2F and G), which is similar to that after MCPH1 deletion. Taken together, these data suggest that MCPH1 regulates mitotic entry in G2 phase via a βTrCP2-mediated degradation of Cdc25A.

To address how MCPH1 promotes Cdc25A degradation, we tested whether MCPH1 deletion would affect the binding between Cdc25A and βTrCP2. Since MCPH1 binds to the substrate interacting domain WD40 of βTrCP2, this may compromise the recruitment of Cdc25A to βTrCP2 for degradation. However, neither knockdown (Fig 2B, IP:FLAG, lanes 2 and 5) nor overexpression (Fig 2C, IP:HA, lanes 8 and 10) of MCPH1 obviously impaired the interaction between βTrCP2 and Cdc25A, indicating that MCPH1 does not mediate the interaction between Cdc25A and βTrCP2. This was further supported by the lack of direct interaction between MCPH1 and Cdc25A (Fig 2C, lanes 9 and 10). Moreover, the knockdown of MCPH1 did not affect the interaction between βTrCP2 and Skp1, the linker of βTrCP2 to the SCF complex (Fig EV2H).

Like other WD domain-containing F-box proteins, while the monomer form harbors the ubiquitination activity, the dimerization can enhance the activity of the SCF complex (Tang *et al*, 2007). We thus hypothesized that a MCPH1-mediated dimerization of βTrCP2 may promote the degradation of Cdc25A. To investigate this, we tagged βTrCP2 and βTrCP1 differently and transfected them into shMCPH1 knockdown cells. Interestingly, the MCPH1 deletion interrupted both the homodimer of βTrCP2 and the heterodimer between βTrCP1 and βTrCP2 (Suzuki *et al*, 2000; Fig 2E). These results indicate that MCPH1 modulates the dimerization of βTrCP2 and is likely to promote the E3 ligase activity of the $SCF^{\beta TrCP2}$ complex toward its substrates.

MCPH1 helps CHK1-independent Cdc25A degradation

It has been shown that in response to DNA damage, the degradation of Cdc25A by βTrCP2 requires a primed phosphorylation of Cdc25A at Ser76 by CHK1 (Jin *et al*, 2003). Moreover, the ATR-CHK1 pathway is compromised in MCPH1 patient cells (Alderton *et al*, 2006). We next asked whether the Cdc25A stability targeted by the MCPH1-βTrCP2 axis is influenced by CHK1-mediated phosphorylation. Indeed, the CHK1 inhibitor UCN-01 only modestly repressed the βTrCP2-induced degradation of Cdc25A (Fig 2F, IB:HA, lanes 2 and 3); however, this partial blockage was not affected by the MCPH1 knockdown (Fig 2F, IB:HA, lanes 5 and 6). To further confirm this, we ectopically expressed a mutant Cdc25A (changing Serine to Aspartic acid at codon 76, Cdc25A-S76D), which mimics a constitutive phosphorylation by CHK1, and found that the MCPH1 knockdown still effectively blocked the βTrCP2-mediated degradation of Cdc25A-S76D (Fig 2G). These data suggest that the MCPH1-βTrCP2 axis plays a major role in the Cdc25A degradation independent of CHK1 and that the function of MCPH1 in DDR is unlikely to be involved in the degradation of Cdc25A.

Overexpression of βTrCP2 or deletion of Cdc25A rescue mitotic entry defects in MCPH1 deficient cells

The major characteristics of MCPH1 patient cells or cells lacking MCPH1 are the high mitotic index and premature chromosome condensation (PCC), which are consequences of an early mitotic entry (Jackson *et al*, 2002; Trimborn *et al*, 2004, 2006; Alderton *et al*, 2006; Gruber *et al*, 2011). To investigate whether the alteration of the βTrCP2-Cdc25A axis is responsible for these defects, we overexpressed βTrCP2 or depleted Cdc25A (mimicking a hyperactivation of βTrCP2), or depleted Cdc25B (as a positive control Gruber *et al*, 2011) in MCPH1-deficient HeLa cells (Fig EV1G, H and I). To measure the mitotic index, we scored the cells expressing the phosphorylation of H3-S10 (pH3-$S10^{+}$), which appears from prepro-phase or late G2 (Fig 3A, Table EV2). We found that consistent with previous studies (Neitzel *et al*, 2002), the MCPH1 depletion increased the amount of preprophase cells, indicative of a premature mitotic entry, whereas an overexpression of βTrCP2 largely corrected the mitotic index defect (Fig 3B and C) and the PCC

© 2017 The Authors

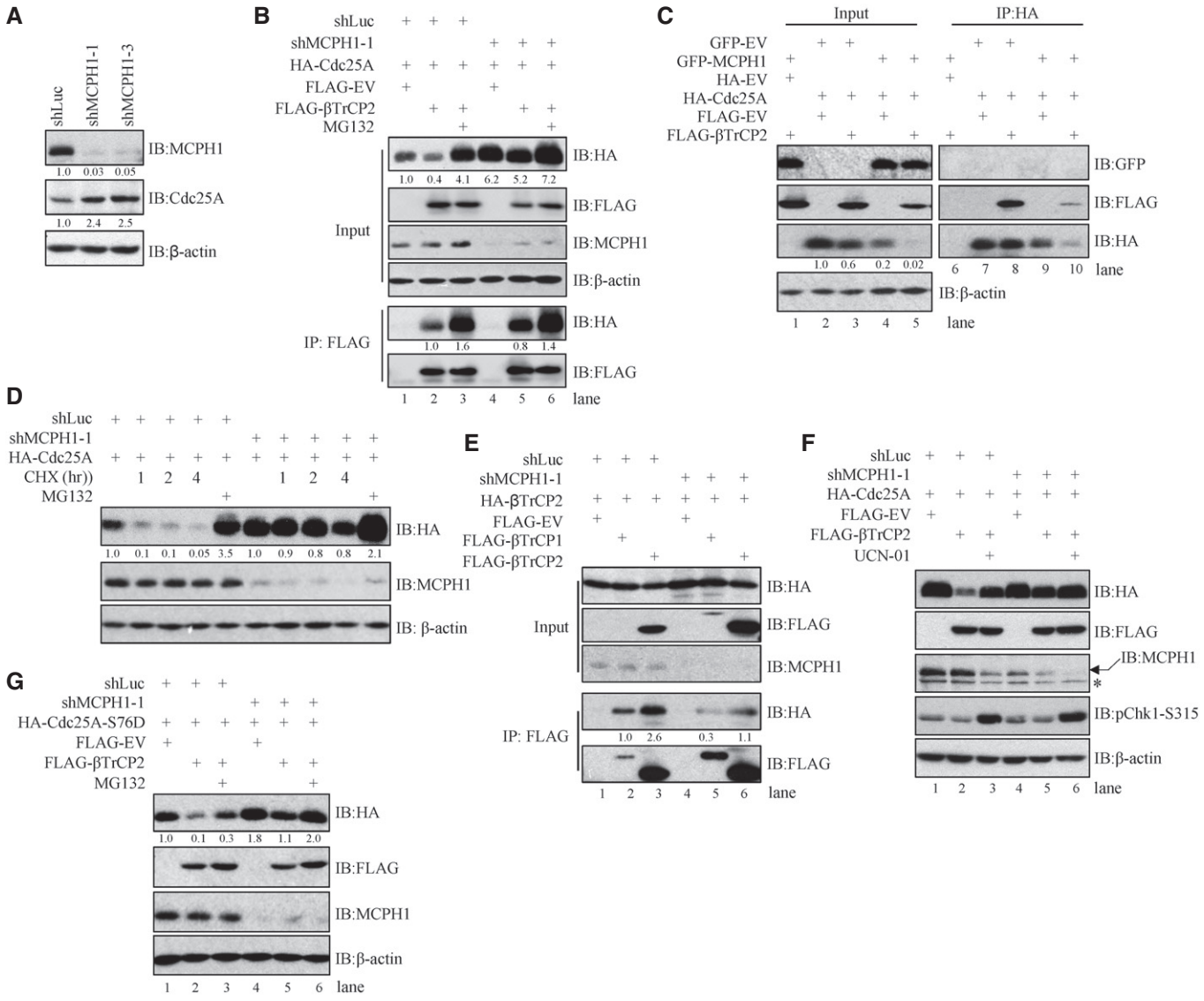

Figure 2. MCPH1 regulates βTrCP2 to degrade Cdc25A.

A Two shRNAs against MCPH1 (shMCPH1-1 and shMCPH1-3) were transfected into 293T cells. The protein level of endogenous MCPH1 and Cdc25A was analyzed by IB using indicated antibodies, respectively. β-actin is used as a loading control. The level of MCPH1 and Cdc25A is a ratio to shLuc after normalization of β-actin of the blots on display. The experiment was repeated three times.

B HA-Cdc25A and FLAG-βTrCP2 were co-transfected into shLuc- or shMCPH1-1-transfected 293T cells. The degradation of Cdc25A (HA) and interaction with βTrCP2 (FLAG) were investigated using the anti-HA antibody. β-actin is used as a loading control. The level of Cdc25A (IB:HA) in Input is normalized to β-actin and shLuc/HA-Cdc25A is set as 1.0. The number under each sample in the immunocomplex (IP:FLAG) is a ratio to shLuc/βTrCP2/Cdc25A (IB:HA) after normalization to Input (IB:HA) of the blots on display. The experiment was repeated twice.

C GFP-MCPH1, FLAG-βTrCP2, and HA-Cdc25A were co-transfected into 293T cells. IP was performed using anti-FLAG antibody. IB was performed using anti-FLAG, anti-HA, or anti-GFP antibody. β-actin is used as a loading control. Input in each panel is 10% of total cell lysates. The level of Cdc25A (in Input IB:HA) is a ratio to HA-Cdc25A (in GFP-EV/FLAG-EV transfected, lane 2) after normalization to β-actin of the displayed blots.

D The stability of HA-Cdc25A was examined after cycloheximide (CHX) treatment for the indicated time in shLuc- and shMCPH1-1-transfected 293T cells and visualized by an anti-HA antibody. β-actin was used to control the loading. The level of HA-Cdc25A after normalization to β-actin is presented as a ratio to untreated shLuc/HA-Cdc25A or shMCPH1/HA-Cdc25A of the blots on display. The experiment was repeated three times.

E Dimer formation of βTrCP2 was examined by co-transfection of HA-βTrCP2 with FLAG-βTrCP1 or FLAG-βTrCP2 in shLuc- or shMCPH1-1-transfected cells. IP was performed using anti-FLAG antibody, and IB was performed using anti-FLAG or anti-HA antibody. The number under each sample in the immunocomplex (IP:FLAG) is a ratio to βTrCP2:βTrCP1 heterodimer (IB:HA) after normalization to Input (IB:HA) of displayed blots.

F HA-Cdc25A and FLAG-βTrCP2 were co-transfected into shLuc- or shMCPH1-1-transfected 293T cells. The degradation of Cdc25A was investigated using the anti-HA antibody. The cells were treated with CHK1 inhibitor (UCN-01) before harvest. β-actin is used as a loading control. The level of Cdc25A (IB:HA) is a ratio to shLuc/HA-Cdc25A after normalization to β-actin. The experiment was repeated three times. Asterisk marks a non-specific band recognized by the anti-MCPH1 antibody.

G HA-Cdc25A-S76D and FLAG-βTrCP2 were co-transfected into shLuc- or shMCPH1-1-transfected 293T cells. The degradation of Cdc25A-S76D was investigated by using anti-HA antibody. β-actin is used as a loading control. The level of Cdc25A is a ratio to shLuc/Cdc25A-S76D (IB:HA) after normalization to β-actin of the blots on display. The FLAG-EV or HA-EV blots are not shown because their size is too small to be included. The experiment was repeated twice.

 © 2017 The Authors

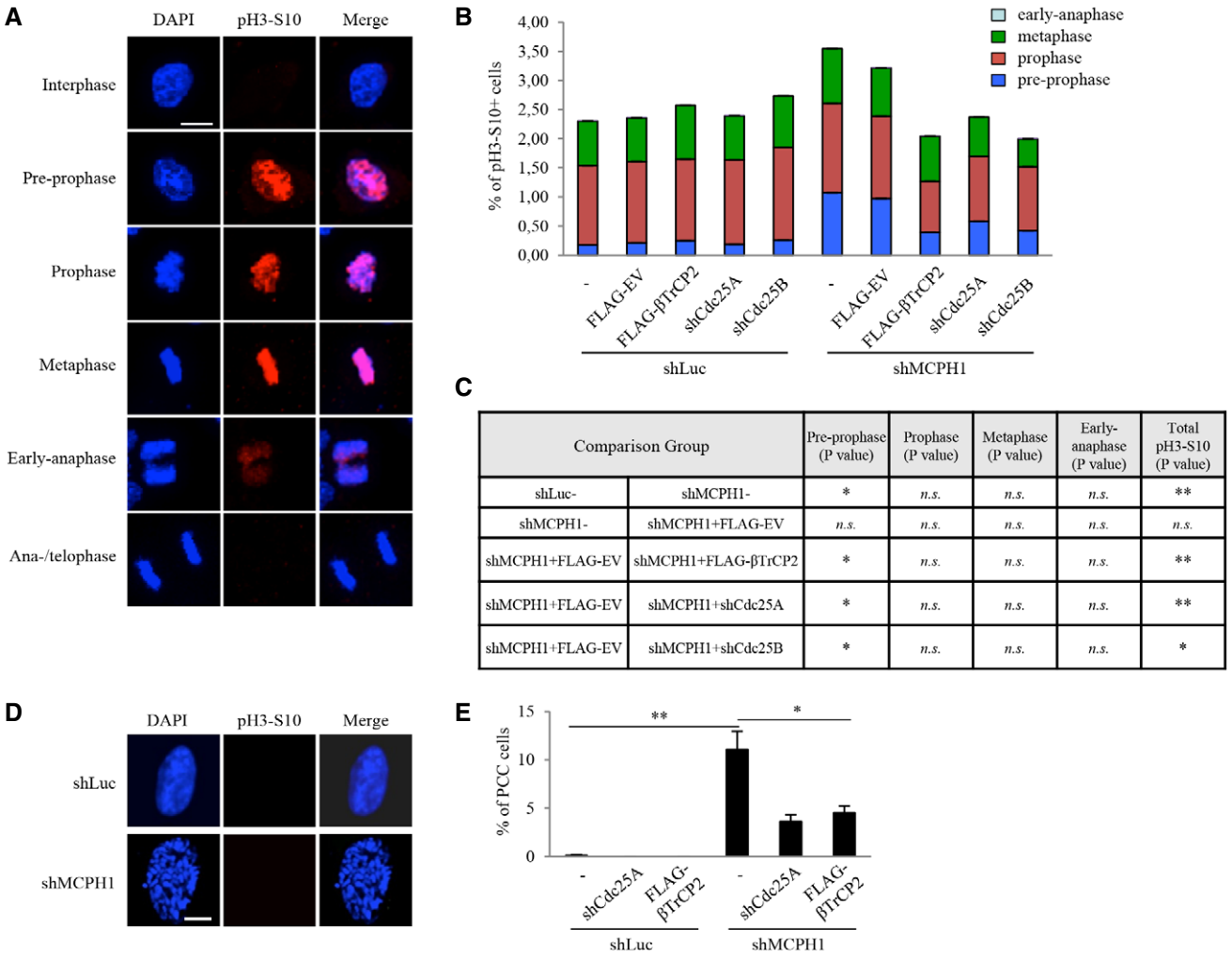

Comparison Group		Pre-prophase (P value)	Prophase (P value)	Metaphase (P value)	Early-anaphase (P value)	Total pH3-S10 (P value)
shLuc-	shMCPH1-	*	*n.s.*	*n.s.*	*n.s.*	**
shMCPH1-	shMCPH1+FLAG-EV	*n.s.*	*n.s.*	*n.s.*	*n.s.*	*n.s.*
shMCPH1+FLAG-EV	shMCPH1+FLAG-βTrCP2	*	*n.s.*	*n.s.*	*n.s.*	**
shMCPH1+FLAG-EV	shMCPH1+shCdc25A	*	*n.s.*	*n.s.*	*n.s.*	**
shMCPH1+FLAG-EV	shMCPH1+shCdc25B	*	*n.s.*	*n.s.*	*n.s.*	*

Figure 3. βTrCP2-mediated mitotic entry after MCPH1 knockdown.

A Representative images of immunofluorescence staining by anti-pH3-S10 in shLuc-transfected cells. Scale bar: 10 μm.

B Quantification of pH3-S10-positive (pH3-S10$^+$) cells in shLuc- or shMCPH1-1-transfected HeLa cells, which were subsequently knocked down for Cdc25A or Cdc25B (positive control), or overexpressed FLAG-βTrCP2.

C Statistical analyses of different sub-phases of the mitosis in the panel (B). Three independent experiments were performed, and more than 1,000 cells were counted per experiment.

D Representative images of normal nucleus of shLuc cells and premature chromosome condensation (PCC) nucleus which show high condensed chromosomes without pH3-S10 staining of shMCPH1 cells after DAPI staining. Scale bar: 10 μm.

E Quantification of PCC containing cells in shLuc- and shMCPH1-transfected HeLa cells, which were subsequently knocked down for Cdc25A or overexpressed βTrCP2. Three independent experiments were performed, and 500 cells were counted per experiment. Error bars represent SD. Statistical analysis was performed by a Student's *t*-test. n.s. = not significant; *$P < 0.05$; **$P < 0.01$.

phenotype (Fig 3D and E) in MCPH1 deficient cells. Moreover, the knockdown of Cdc25A and Cdc25B could also largely correct premature mitotic entry (preprophase defect); however, none of these significantly changed the cell number in prophase and metaphase (Fig 3B and C, Table EV2A). These data indicate that MCPH1 maintains a proper mitotic entry indeed through the βTrCP2-Cdc25A pathway.

MCPH1 is downregulated in late M and G1 phases

MCPH1 is required for a proper mitotic entry. However, stably overexpressing MCPH1 in cells is not possible (Wood *et al*, 2008; Brown *et al*, 2010; Hainline *et al*, 2014). These observations are puzzling, but point out that a fine-tuning of the MCPH1 dynamics is essential for the cell fate. We then analyzed how MCPH1 is regulated during cell cycle progression. First, cells were released from the T-T block, which synchronized cells in the early S-phase (Fig EV3A), and the dynamics of MCPH1 was analyzed by immunoblotting. We found a decline of MCPH1 10–12 h after block release, at which time pH3-S10 was positive, and cyclin B1 and Aurora A reduced, indicatives of M and G1 phases (Figs 4A and EV3A). Consistent with the notion that the thymidine block triggers DNA damage, a high level of phosphorylated CHK1 was detectable at early time points (0–2 h;

© 2017 The Authors

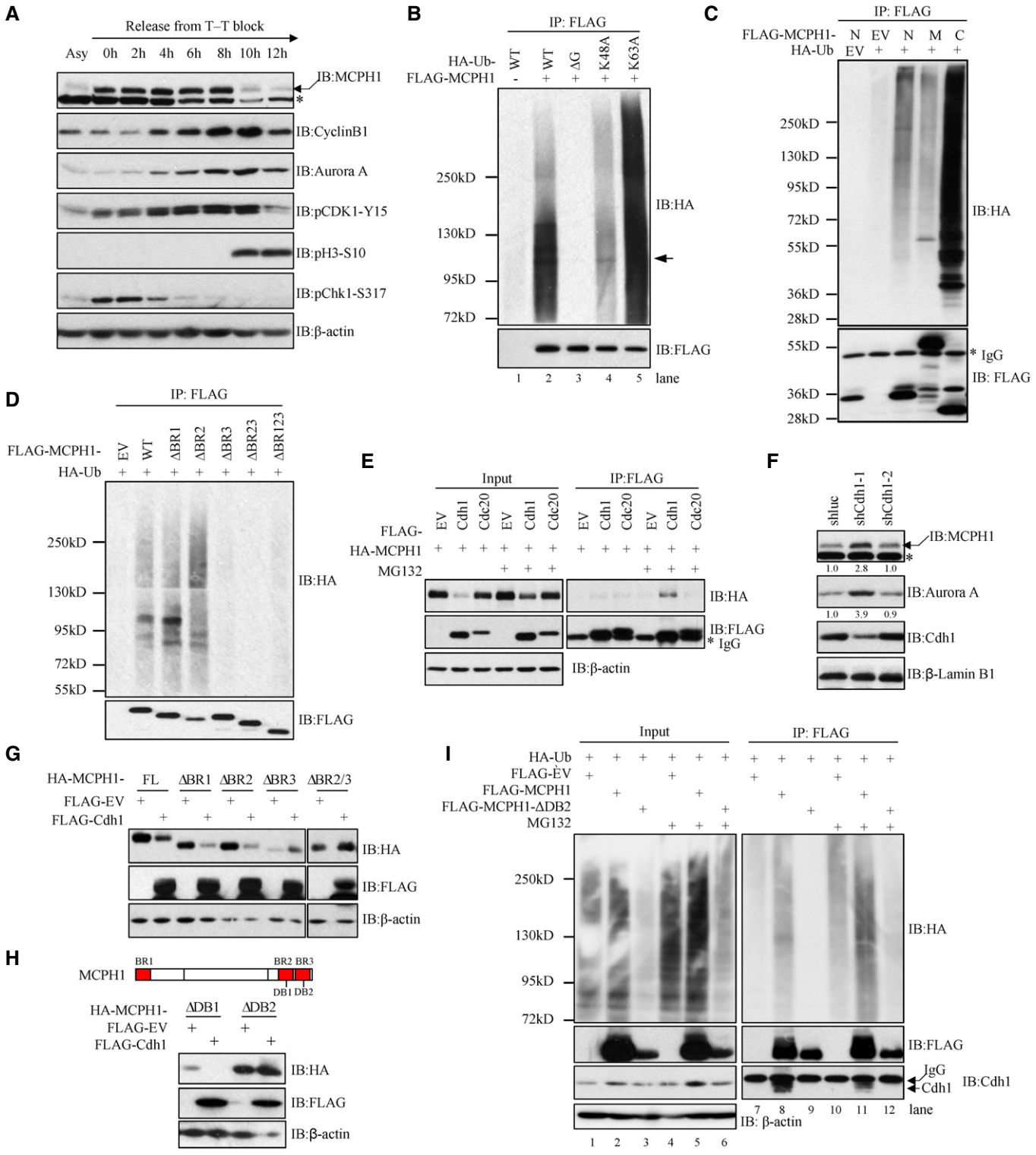

Figure 4.

the S-phase, Figs 4A and EV3A) consistent with its role in S-phase checkpoint. Thus, the decline of the MCPH1 level in M and G1 phases is unlikely due to a DDR from CHK1-mediated S-phase checkpoint, but rather suggests its cell cycle dependent turnover.

MCPH1 is polyubiquitinated *in vivo*

To further investigate whether MCPH1 is degraded via ubiquitination, we co-transfected cells with plasmids expressing HA-tagged ubiquitin (HA-Ub) and FLAG-MCPH1 into 293T cells. As shown in

 © 2017 The Authors

Figure 4. APC/C^{Cdh1}-mediated degradation of MPCH1.

A IB analysis of the MCPH1 protein levels in HeLa cells during G2-M transition at the indicated time after release from S-phase synchronized by double-thymidine (T-T) blockage. pH3-S10 and pCDK1-Y15 were used to mark the M phase entry. β-actin served as a loading control. Asterisk marks a non-specific band recognized by the anti-MCPH1 antibody. The experiment was repeated three times.

B Ubiquitination of MCPH1. FLAG-MCPH1 was co-transfected with constructs expressing HA-tagged ubiquitin wild-type (Ub) and mutant (ΔG, K48A or K63A) into 293T cells. IP was performed using anti-FLAG antibody, and IB was performed using anti-HA or anti-FLAG antibody. The arrow points to the basal position of MCPH1.

C Ubiquitination analysis of 293T cells after co-transfection of FLAG-tagged empty vector (EV), three fragments of MCPH1: N fragment (1–255aa), M fragment (256–633aa), and C-fragment (633–835aa), together with HA-tagged ubiquitin (HA-Ub). IP was performed using anti-FLAG antibody, and IB was performed using anti-HA or anti-FLAG antibody. Asterisk marks the IgG band.

D FLAG-tagged deletion mutants of MCPH1 were co-transfected with HA-Ub. IP was performed using anti-FLAG antibody, and IB was performed using anti-HA or anti-FLAG antibody.

E MCPH1 is degraded by APC^{Cdh1}. HA-MCPH1 was co-transfected with FLAG-EV (empty vector), FLAG-Cdh1 or FLAG-Cdc20 into 293T cells. IP was performed by using anti-FLAG antibody, and IB was analyzed for the MCPH1 protein level using anti-HA antibody. 10% of total lysates was used for input. β-actin serves as a loading control. The experiment was repeated twice. Asterisk marks the IgG band.

F Two shRNAs against Cdh1 (shCdh1-1 and shCdh1-2) were transfected into HeLa cells. The knockdown efficiency of Cdh1 was analyzed using an anti-Cdh1 antibody. After knocking down Cdh1, the level of MCPH1 and Aurora A (positive control) was analyzed using an anti-MCPH1 or Aurora A antibody. Lamin B1 serves as a loading control. The level of MCPH1 and Aurora A is a ratio to shLuc after the normalization of lamin B1 of the blots on display. The experiment was repeated three times. Asterisk marks a non-specific band recognized by the anti-MCPH1 antibody.

G HA-MCPH1 full-length or deletion mutants lacking different BRCT domain were co-transfected with FLAG-EV or FLAG-Cdh1. The protein level of MCPH1 was analyzed using anti-HA antibody. β-actin serves as a loading control.

H The degradation of HA-tagged MCPH1 deletion mutants lacking DB1 (Δ690–696aa) or DB2 (Δ752–759aa) (depicted in upper panel) after transfection with FLAG-EV or FLAG-Cdh1. β-actin was used as a loading control. The FLAG-EV or HA-EV blots are not shown because their size is too small to be included.

I FLAG-MCPH1 or FLAG-ΔDB2 was co-transfected with the construct expressing HA-tagged ubiquitin into 293T cells. IP was performed using an anti-FLAG antibody and IB was performed using the indicated antibodies. The ubiquitination of FLAG-MCPH1 or FLAG-ΔDB2 is visualized by blotting with an anti-HA antibody. Note, IB: Cdh1 detects endogenous Cdh1 which is just below the IgG band (lanes 8 and 11).

Fig 4B, the FLAG-MCPH1 sample showed a smear with a molecular mass much larger than the MCPH1 protein after the anti-HA antibody staining (Fig 4B, lane 2). A deletion of the C-terminal tandem glycine residues (ΔG), which is responsible for the ubiquitin conjugation to the substrates (Hershko & Ciechanover, 1998; Hemelaar *et al*, 2004), completely eliminated the smear pattern (Fig 4B, lane 3). These results indicate that MCPH1 is polyubiquitinated *in vivo*. To determine which type of ubiquitin chain, K48 or K63, the two most common linkage types of polyubiquitin chains, contributes to the MCPH1 polyubiquitination, we co-transfected cells with FLAG-MCPH1 and HA-Ub with either the K48A or the K63A mutation (changing lysine to alanine). The level of MCPH1 ubiquitination was significantly reduced with K48A, but not with K63A, as compared to wild-type (WT) ubiquitin (Fig 4B), indicating that the K48-mediated UPS is mainly involved in the ubiquitination and the degradation of MCPH1. To map which part of MCPH1 was targeted for ubiquitination, different MCPH1 truncations were co-expressed with HA-Ub into 293T cells. We found that the C-terminal MCPH1, containing BRCT2 and BRCT3, was heavily labeled by HA-Ub as compared to the N-terminal or middle part of MCPH1 (Fig 4C). Moreover, a deletion of BRCT3 alone, but not BRCT1 or BRCT2, was sufficient to abolish the MCPH1 ubiquitination (Fig 4D), suggesting that the BRCT3 domain contains ubiquitination sites and is likely to be responsible for the polyubiquitination of MCPH1.

MCPH1 is targeted for degradation by APC/C^{Cdh1}

Since MCPH1 is not a target for the SCF$^{\beta TrCP2}$ complex, we next explored which ubiquitin E3 ligase complex targets MCPH1 for ubiquitination and degradation. Because MCPH1 declines during the M phase, we then turned to test whether MCPH1 is a potential substrate of the APC/C E3 ligase complex, a major ubiquitin E3 ligase in mitosis. To this end, HA-MCPH1 was co-transfected with either FLAG-Cdc20 or FLAG-Cdh1, the two activators of the APC/C complex, into 293T cells. Co-IP showed that HA-MCPH1 could be pulled down by FLAG-Cdh1 but not by FLAG-Cdc20 (Fig 4E). Furthermore, compared to control, the MCPH1 level was dramatically reduced in Cdh1-transfected cells, but not in Cdc20-transfected cells (Fig 4E). In addition, immunofluorescence analysis revealed that MCPH1 was degraded in cells overexpressing Cdh1, but not Cdc20 (Fig EV3B). Reversely, a knockdown of Cdh1 (Fig 4F), but not Cdc20 (Fig EV3C), by shRNA increased the MCPH1 level. Moreover, the downregulation of MCPH1 in Cdh1-transfected cells was partially rescued by the MG132 treatment (Fig 4E). Of note, DNA damage by 10 Gy IR did not further increase the degradation of MCPH1 by Cdh1 (Fig EV3D), suggesting that this event is independent of DDR. Altogether, these data indicate a Cdh1-, but not a Cdc20-mediated degradation of MCPH1 by APC/C.

We next investigated at which cell cycle phase Cdh1 degrades MCPH1. To this end, HeLa cells transfected with shCdh1 or shLuc were synchronized by the T-T block and released for 6 h (G2 phase), 9 h (M phase), and 12 h (mitotic exit or G1 phase; Fig EV4A). We measured the stability of endogenous MCPH1 at different cell cycle phases using CHX. The high level of MCPH1 in shCdh1 cells was seen mainly in G1 phase (Fig EV4B). We also analyzed MCPH1 mRNA at each time point and found that there is no difference of mRNA levels between control shLuc- and shCdh1-transfected cells (Fig EV4C), ruling out the transcriptional influence on the MCPH1 protein level during M and G1 progression.

Consistent with the fact that BRCT3 was required for ubiquitination, the deletion of BRCT3 alone or BRCT2/BRCT3 completely abolished the APC/C^{Cdh1}-mediated degradation of MCPH1 (Fig 4G). The APC/C complex recognizes the KEN box (Lys-Glu-Asn) or the destruction motif named D box (Arg-X-X-Leu-X-X-X-Asn, X represents any amino acids) in the targeted substrate (van Leuken *et al*, 2008). Two sequences similar to D boxes (DB1: Arg-Thr-Leu-Asn; DB2: Arg-Gly-Thr-Leu-Phe-Phe-Ala-Asp-Gln) were found in the C-terminal BRCT2 and BRCT3 of MCPH1, respectively (Fig 4H). A deletion of DB2 in the BRCT3 domain, but not in DB1 in BRCT2,

© 2017 The Authors

abolished the degradation of MCPH1 by Cdh1 (Fig 4H). Moreover, the deletion of DB2 blocked MCPH1 binding to endogenous Cdh1 and abolished the ubiquitination of MCPH1 (Fig 4I, lane 9). Again, 10 Gy IR had no obvious influence on the stability of the DB2 mutant MCPH1 in the presence of ectopic Cdh1 (Fig EV3D, lanes 16–19). These data suggest that the MCPH1 degradation mediated by Cdh1 is likely DDR independent. These data indicate that the MCPH1 stability is regulated through the DB2 in the BRCT3 domain by APC/C^{Cdh1} under physiological condition as well as upon DNA damage.

Failure of degradation of MCPH1 blocks cell division and induces cell death

To understand the biological meaning of the MCPH1 degradation in the M phase, we performed a live cell imaging to follow up the fate of U2OS cells that ectopically express GFP-EV or GFP-MCPH1. The aim of this experiment was to investigate the consequence when the MCPH1 level is forced to present during mitosis. An overexpression of MCPH1 (GFP-MCPH1) blocked cell division (Fig 5A and B). This was further confirmed by a dramatically decrease of pH3-Ser10-positive cells in GFP-MCPH1 population as compared to GFP-EV controls (Fig 5C). Intriguingly, most of the GFP-MCPH1 cells died during a live cell imaging period of 48 h (Fig 5A and B). A FACS analysis also revealed an increase of the Annexin V-positive population in cells overexpressing MCPH1 (Fig 5D) and a high percentage of sub-G1 cells (Fig 5E and F), both of which are indicative of cell death. Despite our major efforts and attempts, we failed to establish any stable cell lines with an ectopic expression of MCPH1, which is consistent with the notion that an overexpression of MCPH1 is toxic to cells seen by others (Wood *et al*, 2008; Brown *et al*, 2010; Hainline *et al*, 2014). Similarly, an overexpression of non-degradable MCPH1-ΔBR2 also blocked cell division and induced cell death (Fig 5A, B and G), mimicking the forced expression of wild-type MCPH1. These data indicate that a proper turnover of MCPH1 is important for cell cycle progression and cell survival.

Ectopic expression of βTrCP2 or Cdh1 modulates the cell fate of neuroprogenitors in *Mcph1*-del cortex

We showed previously that a knockout of MCPH1 results in microcephaly due to a biased neurogenic differentiation of neuroprogenitors and a premature mitotic entry of *Mcph1*-del neuroprogenitors (Gruber *et al*, 2011). We next investigated whether the MCPH1-βTrCP2-Cdc25A pathway is ultimately responsible for neuro-stem cell mitotic entry and thereby cell fate determination during neurogenesis *in vivo*. To this end, we employed the *in utero* electroporation (IUE) technique and overexpressed GFP-EV, GFP-βTrCP2, or GFP-βTrCP2ΔN (deletion of N-terminal βTrCP2 and dimerization mutant) in the *Mcph1*-del neocortex at E14.5 (Fig 6A). We first analyzed the mitotic entry of neuroprogenitors *in vivo* 2 days later in E16.5 brain sections by scoring the number of pH3-$S10^+$ cells in transfected neuroprogenitors (GFP^+). We found that consistent with the cell line data (Fig 3B), βTrCP2 overexpression repressed the abnormally high mitotic entry of *Mcph1*-del neuroprogentors (Fig 6B and C). The differentiation capacity was further analyzed by measuring the cell cycle exit index (percentage of GFP^+Ki67^- vs. all GFP^+ cells) in the neocortex at E16.5 after staining for Ki67, a marker for proliferating cells. Consistent with our previous study, the *Mcph1*-del neocortex showed a higher cell cycle exit index compared to control animals (Gruber *et al*, 2011; Fig 6D and E), indicating a premature differentiation. An overexpression of βTrCP2 ameliorated the abnormally high cell cycle exit index in the *Mcph1*-del brain to the level of control wild-type animals (Fig 6D and E, Table EV3A). An overexpression of the dimer-deficient βTrCP2ΔN could not degrade Cdc25A (Fig EV5A) and could, but with a less efficiency, correct the high cell cycle exit index (Fig 6E), suggesting that dimerization may not be essential, but contributes to the βTrCP2 activity *in vivo*.

Moreover, an overexpression of Cdh1 by IUE enhanced cell cycle exit index in wild-type neuroprogenitors (Fig 6F and G, Table EV3B), mimicking neuroprogenitor premature differentiation in *Mcph1* mutant mice. This defect was analyzed by scoring Sox2 (a neuroprogenitor marker) expressing cells and confirmed by a high percentage of GFP^+Sox2^- present in all GFP^+ *Mcph1*-del neuroprogenitors after an ectopic expression of Cdh1 (Fig EV5B, Table EV3C). Finally, an ectopic expression of Cdh1 did not change the cell cycle exit of the *Mcph1*-del neuroprogenitors (Fig 6F and G, Table EV3B), suggesting that MCPH1 and Cdh1 operate in the same pathway. These observations indicate again that a proper MCPH1 level is important to control neuroprogenitor differentiation.

Discussion

The cell fate decision of neuroprogenitors is highly influenced by the cell cycle progression (Arai *et al*, 2011; Cheffer *et al*, 2013; Tapias *et al*, 2014). In the current study, we show that the modulation of MCPH1 homeostasis by APC/C^{Cdh1}- and MCPH1-mediated βTrCP2 activity are a concerted action that is required for proper cell cycle progression. We further demonstrate that an overexpression of βTrCP2 can counterbalance MCPH1 deficiency-induced neuroprogenitor premature differentiation. We hence built a network involving the protein kinetics of the Cdh1-MCPH1-βTrCP2-Cdc25A axis and demonstrated an operational mechanism in maintaining neurogenesis and preventing microcephaly (Fig EV6).

The ubiquitin E3 ligase $SCF^{\beta TrCP}$ and APC/C^{Cdh1} complexes cooperate with each other to ensure a proper cell cycle transition (Vodermaier, 2004; Choudhury *et al*, 2016). Whereas $SCF^{\beta TrCP}$ is important for the S-phase progression and G2-M transition, APC^{Cdh1} is activated in late mitosis and secures G1 phase (van Leuken *et al*, 2008). These two UPS complexes share common substrates during cell cycle progression. For example, Cdc25A is degraded by APC/C^{Cdh1} in the mitotic exit and early G1 phase, while $SCF^{\beta TrCP}$ is required for the degradation of Cdc25A in the S and G2 phase, likely compensating for the low activity of APC/C^{Cdh1} in the interphase (Donzelli *et al*, 2002). The delicate availability of different UPS systems allows a choice of specific interaction partners, either promoters or substrates, to be used to ensure proper cell cycle progression. Intriguingly, MCPH1 interacts with both βTrCP2 and Cdh1 linking both UPS systems, both of which regulate MCPH1's function and fate in a cell cycle specific manner: to ensure a proper M phase entry by stimulating the $SCF^{\beta TrCP2}$ activity and to secure the mitosis exit and G1 progression. MCPH1 is a target for APC/C^{Cdh1}-mediated degradation (otherwise it is

 © 2017 The Authors

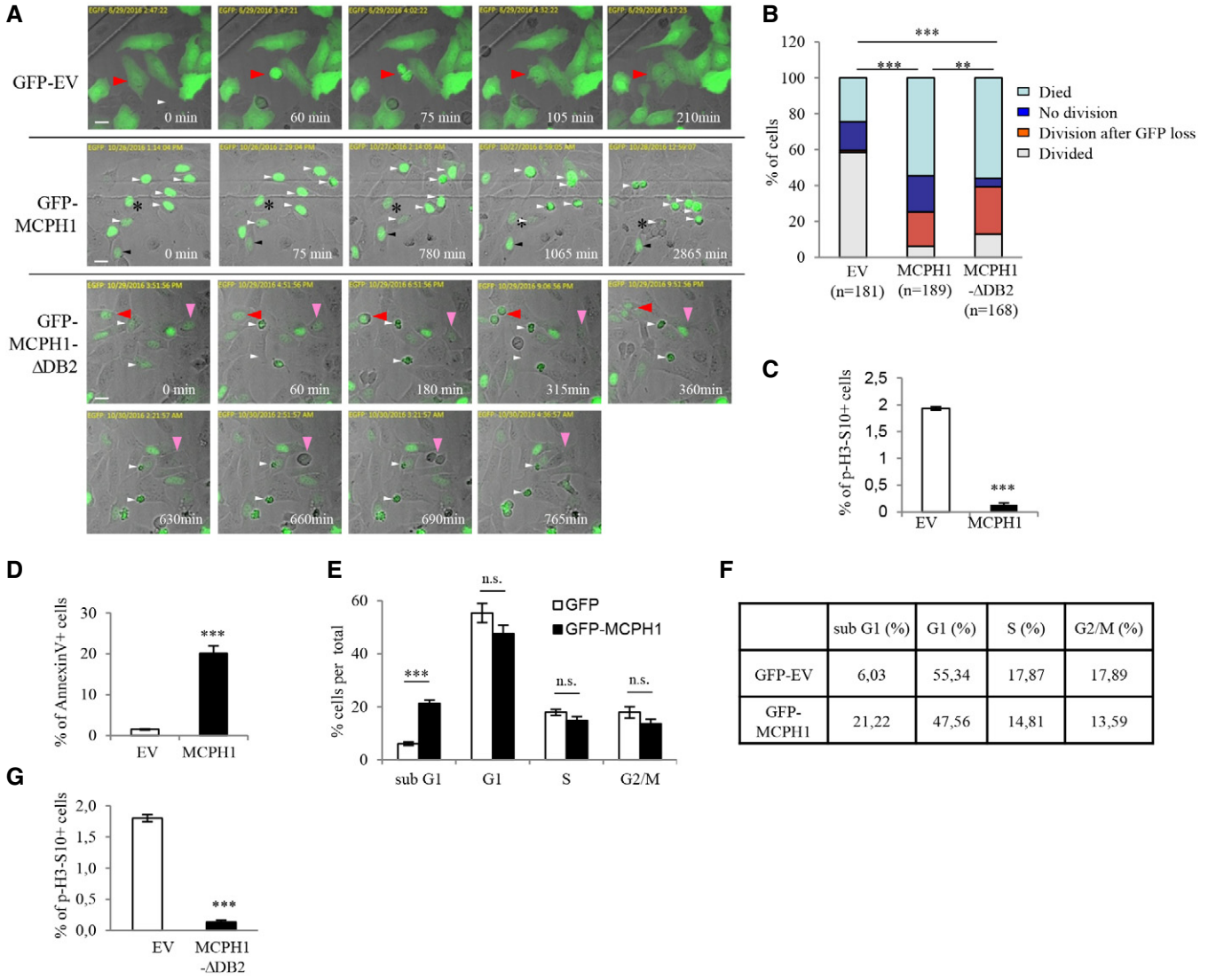

	sub G1 (%)	G1 (%)	S (%)	G2/M (%)
GFP-EV	6,03	55,34	17,87	17,89
GFP-MCPH1	21,22	47,56	14,81	13,59

Figure 5. Overexpression of MCPH1 blocks cell division and induces cell death.

A Live cell imaging analysis of U2OS cells after transfection with the indicated vectors. Cells were recorded for 48 h. Red arrow: dividing cell; white arrowhead: dead cell; black arrowhead or asterisk: block in division; pink arrow: divided cells after GFP signal loss. The acquisition time is shown at the top (yellow); the relative time is shown at the bottom right (white). Scale bar: 20 μm.

B The percentage of GFP-positive cells in different categories is shown. *n*: total number of cells. A chi-square test was performed for statistical analysis. $^{**}P < 0.01$; $^{***}P < 0.001$.

C Quantification of mitotic (pH3-S10-positive) cells in GFP-EV- or GFP-MCPH1-transfected HeLa cells by FACS analysis. Three independent experiments were performed. Error bars represent SD. Statistical analysis is performed by Student's *t*-test.

D Quantification of Annexin V-positive cells in GFP-EV- or GFP-MCPH1-transfected HeLa cells by FACS analysis. Three independent experiments were performed. Error bars represent SD. Statistical analysis is performed by Student's *t*-test. $^{***}P < 0.001$.

E FACS analysis of cell cycle profile of GFP-EV- and GFP-MCPH1-transfected HeLa cells. The experiment was repeated three times. Error bars represent SD. Statistical analysis was performed using Student's *t*-test. $^{***}P < 0.001$.

F The distribution of each cell cycle phase is summarized in the table.

G Quantification of mitotic (pH3-S10-positive) cells in GFP-EV- or GFP-MCPH1-ΔDB2-transfected HeLa cells by FACS analysis. Three independent experiments were performed. Error bars represent SD. A statistical analysis is performed by Student's *t*-test. $^{***}P < 0.001$.

cytotoxic). The activity of Cdh1 is inhibited in S and G2 by binding to Eim1, whose degradation by $SCF^{\beta TrCP}$ releases Cdh1 to allow cells progress through mitosis (Margottin-Goguet *et al*, 2003). It seems that $SCF^{\beta TrCP2}$ is a key protein to coordinate G2-M transition. It is conceivable that on one hand βTrCP2, with help of MCPH1, degrades Cdc25A to grant a mitotic entry and on another hand degrade Eim1 to activate Cdh1 that degrades MCPH1 when cells is entering mitosis, failure which otherwise blocks M-G1 transition and triggers cell death. These coordinated actions seem to play a key role in regulating cell cycle progression, which dictates the division mode and the fate of neural stem cells (Fig EV6).

© 2017 The Authors

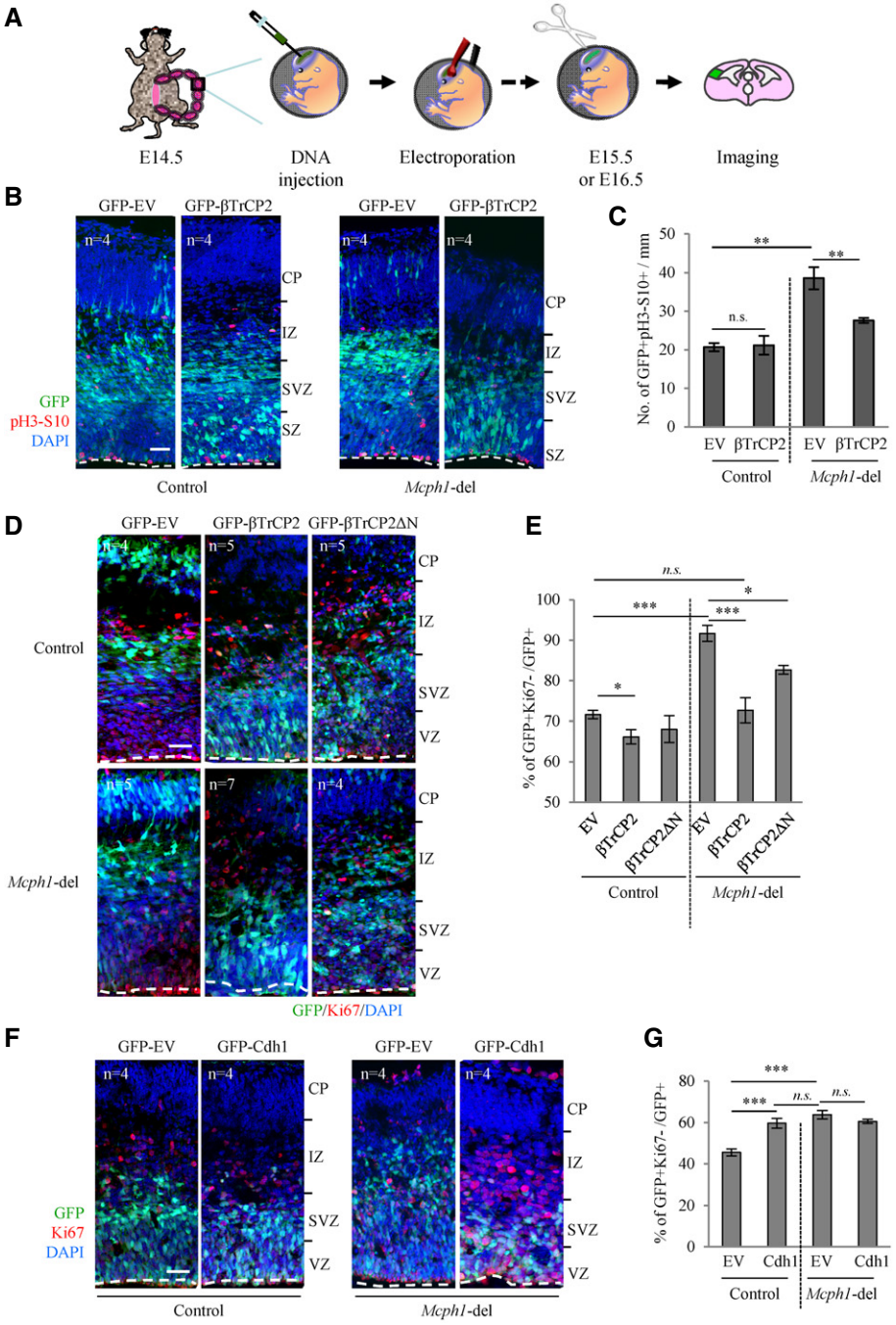

Figure 6. Overexpression of βTrCP2 and Cdh1 in *Mcph1*-del neocortex.

A Schemes depict the *in utero* electroporation protocol. GFP-tagged expressing vectors of interest are electroporated into wild-type or *Mcph1*-del embryonic brain ventricles at E14.5. The embryonic brain is analyzed by imaging at the indicated time. Immunofluorescence staining of brain sections is performed using antibodies.

B Representative images of pH3-S10 staining of E16.5 brain sections after GFP-EV or GFP-βTrCP2 transfection. *n*: number of embryos analyzed. Scale bar: 50 μm. VZ, ventricular zone; SVZ, subventricular zone; IZ, intermediate zone; CP, cortical plate.

C Quantitation of the number of $GFP^+pH3\text{-}S10^+$ cells per 1 mm area. Error bars represent the SD. Statistical analysis was performed using one-way ANOVA. $^{**}P < 0.01$.

D Representative images of Ki67 staining at E16.5 brain sections after GFP-EV, GFP-βTrCP2, GFP-βTrCP2ΔN transfection. *n*: number of embryos analyzed. Scale bar: 50 μm. VZ, ventricular zone; SVZ, subventricular zone; IZ, intermediate zone; CP, cortical plate.

E Quantitation of GFP^+Ki67^- cells per total GFP^+ cells. For each embryo, at least 1,500 GFP^+ cells were counted. Error bars represent SD. Statistical analysis was performed using one-way ANOVA. $^{*}P < 0.05$; $^{***}P < 0.001$.

F Representative images of Ki67 staining at E15.5 brain section after GFP-EV, GFP-Cdh1 transfection. *n*: number of embryos analyzed. Scale bar: 50 μm. VZ, ventricular zone; SVZ, subventricular zone; IZ, intermediate zone; CP, cortical plate.

G Quantitation of GFP^+Ki67^- cells per total GFP^+ cells. For each embryo, at least 2,000 GFP^+ cells were counted. Error bars represent SD. Statistical analysis was performed using one-way ANOVA. $^{***}P < 0.001$.

© 2017 The Authors

We discover that MCPH1 interacts with and promotes the E3 ligase βTrCP2 by facilitating its dimerization to degrade Cdc25A. MCPH1 has been shown to regulate the Cdc25A-Cdk1 pathway through ATR-CHK1 in response to DNA damage (Alderton *et al*, 2006), and MCPH1 regulates the G2-M transition by damping out CHK1 from the centrosome in the G2 phase of neuroprogenitors (Gruber *et al*, 2011). The current study shows that the CHK1 inhibitor did not protect the Cdc25A stability in shMCPH1-knockdown cells and that the CHK1-phosphorylation mimic mutant Cdc25A-S76D is refractory to the βTrCP2-mediated degradation (Fig 2F and G). Thus, MCPH1 controls mitotic entry by modulating $SCF^{\beta TrCP2}$ to target Cdc25A in both CHK1-dependent and CHK1-independent manner. It is known that MCPH1 is involved in DDR (Xu *et al*, 2004; Lin *et al*, 2005; Alderton *et al*, 2006; Rai *et al*, 2006; Wood *et al*, 2008). Interestingly, we found that only a high dose of IR induced MCPH1 degradation (Figs 1E and EV3D) although the nature of the degradation is currently unknown. Nevertheless, DNA damage does not affect the stability of the interaction of between MCPH1 and βTrCP2 (Fig 1B). It is unlikely that the MCPH1-βTrCP2-mediated Cdc25A degradation is due to DDR or cell cycle checkpoint activation.

MCPH1 interacts specifically with βTrCP2, but not with βTrCP1, or other components of the SCF complex, such as FBW7, an F-box protein with a WD40 domain (Welcker & Clurman, 2008), Skp2, another F-box protein containing a leucine-rich interaction domain rather than the WD domain (Bassermann *et al*, 2008), as well as Skp1 (Fig 1D), the adaptor of the $SCF^{\beta TrCP2}$ complex. Moreover, the MCPH1 deletion does not disrupt the partnership between Skp1 and βTrCP2 (Fig EV2H). Therefore, MCPH1 is unlikely to be an authentic component of the SCF complex and it is also most likely not required for the maintenance of the complex. The selective interaction of MCPH1 with βTrCP2, but not with βTrCP1, is striking because βTrCP1 shares an 85% overall similarity with β-TrCP2.

The meaning of this specific interaction is perhaps that MCPH1 binding to βTrCP2 promotes its dimerization. It has been described for other SCF complex proteins that the dimerization, which is however not essential, boosts its activity (Suzuki *et al*, 2000; Tang *et al*, 2007). In this regard, a depletion of MCPH1 compromises the βTrCP2 dimerization (Fig 2E) and concurrently repressed the Cdc25A degradation (Fig 2B and D). Reversely, an overexpression of MCPH1 enhanced the Cdc25A degradation, which is further boosted by the overexpression of βTrCP2 (Fig 2C). How MCPH1 modulates the βTrCP2:βTrCP2 dimer formation and efficiently engages Cdc25A in the βTrCP2-Cdc25A complex remains unknown at this stage. It is possible that MCPH1 binds to the WD40 domain and functions as a scaffold to recruit two βTrCP2s close enough to promote the dimerization. However, our data could not establish the absolute necessity for the dimerization-dependent activity of βTrCP2 toward Cdc25A, because the dimerization mutant βTrCP2 (βTrCP2ΔN) can partially rescue the premature mitotic exit of *Mcph1*-del neuroprogenitors, albeit at a less efficiency than wild-type βTrCP2 (Fig 6E).

Intriguingly, we found that the MCPH1 protein must be tightly regulated in a cell cycle specific manner by the UPS system. MCPH1 regulates the Cdc25A turnover by engaging βTrCP2 in G2 phase to regulate G2-M transition. Since overexpression of MCPH1 blocks the cell division and triggers cell death, MCPH1 must be downregulated at the mitosis or its progression. However, it is unclear how a sustained expression of MCPH1 is toxic to cells. It is interesting to note two recent publications showing that the overexpression of MCPH1 inhibits cell proliferation by promoting apoptosis (Zhou *et al*, 2016) and activating the cytochrome c-caspase 3 signaling (Mai *et al*, 2014). The ubiquitination of MCPH1 is realized by a direct interaction of MCPH1 with Cdh1 and also possibly by an interaction with the scaffold component Cdc27 of APC/C (Singh *et al*, 2012). Of note, the *Drosophila* MCPH1-B isoform, which contains additional 47 amino acids in the N-terminus, but lacks BRCT2 and BRCT3 at the C-terminus compared to human full-length MCPH1, can be degraded by the APC/C^{Cdh1} complex, via a disruptive D box present in the N-terminus. However, we identified the DB2 box in the extreme C-terminus of human MCPH1 as the main target for the degradation by human APC/C^{Cdh1} (Fig 4H). This species specificity may explain why the human MCPH1 cannot be degraded in Cdh1-supplemented *Xenopus* egg extract (Hainline *et al*, 2014).

Despite several substrates of APC/C^{Cdh1} have been identified to ensure a proper cell cycle progression (Bassermann *et al*, 2008; van Leuken *et al*, 2008; Fasanaro *et al*, 2010), the current study identifies MCPH1 as a novel substrate of APC/C^{Cdh1}, particularly in mitotic exit and G1 phase. The biological implication of the APC/C-mediated MCPH1 degradation is to ensure a proper neurogenesis. In this regard, a deletion of Cdh1 in the mouse brain delayed embryonic neurogenesis, which is likely due to a delay of the cell cycle exit of neuroprogenitor cells to produce post-mitotic neurons (Delgado-Esteban *et al*, 2013). In agreement with this study, a forced expression of Cdh1 drives a premature cell cycle exit of neuroprogenitors *in vivo* (Fig 6G). These phenotypes reversely correlate well with our previous findings showing that a deletion of MCPH1 leads to a premature cell cycle exit and enhances neurogenic production leading to microcephaly (Gruber *et al*, 2011; see model in Fig EV6). In addition, an ectopic expression of Cdh1 did not further worsen the cell cycle exit of the *Mcph1*-del neuroprogenitors (Fig 6G), suggesting that MCPH1 and Cdh1 operate in the same pathway. Taken together, these results demonstrate that the APC/C^{Cdh1} complex plays an important role in neurogenesis and cortical development, likely by regulating the turnover of MCPH1 in the cell cycle progression.

We show that MCPH1, on the one hand, regulates the stability of the cell cycle regulator Cdc25A by promoting the degradation activity of its upstream E3 ligase βTrCP2 in interphase and that MCPH1, on the other hand, has to be turned off by the APC/C^{Cdh1} complex in the M-G1 phase; otherwise, it is toxic to the cells. This concerted action ensures proper neuroprogenitor differentiation and thereby brain development.

Materials and Methods

Mice

Mice carrying the *Mcph1* deleted allele (Gruber *et al*, 2011) were maintained in the SPF facility. The *Mcph1* genotypes of the mice were determined by PCR on DNA extracted from tail tissue as previously described. All animal experiments were conducted according to the German animal welfare legislation.

© 2017 The Authors

Yeast two-hybrid (Y-2-H) assays

A yeast two-hybrid screening was performed using the Match-Maker 3 two-hybrid system (Clontech, CA, USA) following the manufacturer's instruction. Briefly, a cDNA fragment encoding a polypeptide of the 96–612AAs of human MCPH1 (ref. sequence: NP_078872), in which all the three BRCT domains were removed, was subcloned into the bait vector pGBKT7, and a pretransformed Matchmaker human cDNA library (Clontech) was used for screening.

Cell lines

HEK293T, HeLa, U2OS, and Neuro 2A cell lines were maintained in Dulbecco's modified Eagle's medium supplemented with 10% fatal bovine serum, 2 mM glutamine, 1 mM sodium pyruvate, β-mercaptoethanol, 50 units/ml penicillin, and 50 mg/ml streptomycin at 37°C in a CO_2 incubator with 20% O_2.

Vectors

The vectors pcDNA-3.0-HA, pcDNA-3.0-FLAG, pcDNA-3.0-HA-MCPH1-FL, pcDNA-3.0-HA-Cdc25A, pcDNA-3.0-FLAG-Cdh1, pcDNA-3.0-HA-MCPH2, pcDNA-3.0-HA-ubiquitin plasmids were constructed. The CAG-driven GFP overexpressing vectors pCAG-GFP were a gift from Connie Cepko (Addgene plasmid # 11150, Cambridge, MA, USA; Matsuda & Cepko, 2004), and the mCherry-H2B was a gift from Michael Davidson (Addgene plasmid # 55056; Kuipers *et al*, 2011). The cDNA of MCPH1, Cdc25A, βTrCP1, βTrCP2, FBX2, FBXW7, Skp1, and Skp2 was produced from HeLa mRNA. To introduce deletion mutations in MCPH1 and βTrCP2, a Quickchange XL Site-Directed Mutagenesis Kit (Stratagene, Frankfurt, German) was used.

shRNA and siRNA

The control siRNA-A (#sc-37007), Cdc25A siRNA (#sc-29254), and Cdc25B siRNA (#sc-37552) were purchase from Santa Cruz, Heidelberg, Germany. The siCdc20-1: Sense 5′-AAACCUGGCGGUGACCG CUAU-3′ and siCdc20-2: Sense 5′-AAUGUGUGGCCUAGUGCUCCU-3′ were synthesized in Eurofins Genomics (Jena, Germany). The construction of shRNA expression vectors was carried out as previously described (Zhou *et al*, 2010). All oligonucleotides contained the hairpin loop sequence 5′-TTCAAGAGA-3′. The targeting sequences are

shLuciferase: 5′-GGCTTGCCAGCAACTTACA-3′;
shMCPH1-1: 5′-GCACACAGAACAAAGGTACCA-3′;
shMCPH1-3: 5′-GCAGAATGTCGTCATCCAGGT-3′;
shβTrCP1-1: 5′-GGCCGAGGCGGTGCTGCAAGA-3′;
shβTrCP1-2: 5′-GGAAGATAATACCAGAGAAGA-3′;
shβTrCP2-1: 5′-GGATGTGAACACGGGTGAAG-3′;
shβTrCP2-3: 5′-GCGCACATTGGTGGAACATTC-3′;
shCdc25A-1: 5′-GGACAGCTCCTCTCGTCATGA-3′;
shCdc25A-2: 5′-GCTGGGAAACATCAGGATTTA-3′.
shCdc25B-1: 5′-GGAGATTACTCTAAGGCCTTC-3′
shCdc25B-2: 5′-GCCTTCAAGGATGAGCTAAAG-3′
shCdh1-1: 5′-GGGACGCAGCCGCAGGGAAGA-3′
shCdh-2: 5′-GCACAGCTGACCGCTGTATCC-3′

qRT–PCR assay

The total RNA was isolated from cells using Tri-Reagent (Sigma-Aldrich, Hamburg, Germany). cDNA was synthesized using Super-Script® III Reverse transcriptase (Invitrogen, Darmstadt, Germany). The real-time quantitative PCR (qRT–PCR) was performed in triplicate for each sample using Platinum SYBR Green qPCR SuperMix-UDG and a CFC96 Touch™ Real-Time PCR Detection System (Bio-Rad, Munich, Germany). The primers for MCPH1, Cdc25A and β-actin were synthesized according to a previous publication (Weischenfeldt *et al*, 2008; Yamashita *et al*, 2010; Gavvovidis *et al*, 2012).

Transfection of cells

The transfection of HEK293T cells was performed with polyethylenimine (PEI, Polyscience, Eppelheim, Germany) at a ratio of 1 μg plasmid per 3 μg PEI. For HeLa cells, the transfection was performed with Lipofectamine® 2000 (Invitrogen) at a ratio of 1 μg plasmid per 3 μl Lipofectamine® 2000. The cells were harvested 48 h after transfection for analysis.

Treatment of cells

The cells were treated with 10 μM MG132 (Sigma-Aldrich) for 4 h or with 100 μg/ml cycloheximide (Sigma-Aldrich) or irradiated [Gammacell 40 (GC40) Irradiator] for different time periods. After the treatment, the cells were harvested in a NETN buffer [50 mM Tris–HCl (pH 7.5), 250 mM NaCl or 150 mM NaCl, 5 mM EDTA, 0.5% NP-40, and a protease inhibitor cocktail (Roche, Berlin, Germany)].

Synchronization of cells

For the cell synchronization, we followed a previous protocol (Busino *et al*, 2003) with minor modifications. Briefly, to block cells in the early S-phase by a double-thymidine block, HeLa cells were treated with 2 mM thymidine (Sigma-Aldrich) for 18 h and then incubated with a fresh medium for 9 h, before the second thymidine incubation for another 17 h. For the stability assay, cells were transfected by shRNAs 4 h before synchronization and were treated with 100 μg/ml cycloheximide (CHX; Sigma-Aldrich) for different time periods at the indicated time point after releasing from synchronization.

Immunoprecipitation and immunoblotting

For immunoprecipitation, 2 μg of the antibodies was incubated with 1 mg of total lysate together with the protein A Sepharose™ CL-4B or the protein G Sepharose™ 4 fast flow (GE Healthcare, München, Germany) at 4°C overnight. The precipitates were washed with the NETN buffer without protease inhibitors. The immunoblots on nitrocellulose or PVDF were blocked with 5% non-fat milk in TBST (TBS with 0.1% Tween 20) and washed in TBST. The antibodies used for immunoblotting are as below: rabbit anti-HA (1:5,000, A190-208A, Bethyl, Hamburg, Germany); mouse anti-FLAG M2 (1:5,000, F-1804, Sigma-Aldrich); mouse anti-GFP (1:1,000, #sc-9996, Santa Cruz); mouse anti-β-actin

 © 2017 The Authors

(1:5,000, #T4026, Sigma-Aldrich); mouse anti-GAPDH (1:5,000, G8795, Sigma-Aldrich); rabbit p-CDK1-Y15 (1:1,000, #4539S, Cell Signaling, Frankfurt, Germany); rabbit anti-MCPH1 (1:500, # 4120, Cell Signaling); rabbit anti-FBXW11 antibody βTrCP2 (1:300, #13149-1-AP, Proteintech, Manchester, UK); rabbit anti-Cdc25A (1:200, ab991, Abcam, Cambridge, UK); mouse anti-Cdc25A (1:200, #sc-7389, Santa Cruz); rabbit anti-Cdc25B (1:1,000, # sc-326, Santa Cruz); rabbit anti-Aurora A (1:300, #603301, Biolegend, Aachen, Germany); mouse anti-cyclin B1 (1:1,000, #554176, BD Pharmingen, Heidelberg, Germany); mouse anti-Cdh1/FZR1 (1:500, # ab3242, Abcam); mouse anti-Chk2 (1:1,000, #05-649, Millipore, Darmstadt, Germany); rabbit phospho-Chk1 (Ser317) antibody (1:500, #2344P, Cell Signaling); rabbit anti-pH3-S10 (1:500, #A301-844A, Bethyl); mouse anti-Cdc20 (1:500, SC-13162, Santa Cruz); goat anti-lamin B1 (1:1,000, #sc-6217, Santa Cruz); goat anti-rabbit immunoglobulin HRP (1:5,000, P0448, DAKO, Hamburg, Germany); goat anti-mouse immunoglobulin HRP (1:5,000, P0447, DAKO).

Immunofluorescence staining of cells and brain sections

The cells were cultured on coverslips, washed with ice-cold PBS, and fixed with ice-cold methanol for 5 min. The samples were blocked with 5% bovine serum albumin (BSA) in PBST (PBS with 0.1% Tween 20) for 30 min at room temperature followed by incubation with rabbit anti-pH3-S10 (1:500, #A301-844A, Bethyl) for 1.5 h and washing with PBST. For the staining of the cryosections of the mouse brain, the antigen was retrieved by using a 10 mM sodium citrate buffer (pH 6.0) and blocked in a blocking solution (5% goat serum, 1% BSA, 0.4% Triton X-100 in PBS). The sections were incubated with the rabbit anti-Ki67 (1:200, Neomarkers, Waltham, MA, USA) or rabbit anti-Sox2 (1:200, # ab97959, Abcam), or with rabbit anti-pH3-S10 (1:500, #A301-844A, Bethyl), at 4°C overnight and washed with PBS. Both coverslips and sections were incubated with the secondary antibody anti-rabbit IgG' fragment-Cy3 (1:200, C2306, Sigma-Aldrich) for 2 h. The DNA was counterstained with DAPI (4′,6-diamidino-2-phenylindole).

Flow cytometry analysis

The cells were collected at different time points after synchronization or 48 h after transfection with GFP-MCPH1 or GFP-MCPH1-ΔDB2, resuspended with cold PBS, and fixed in a fixation solution (2% glucose, 3% paraformaldehyde in PBS) on ice for 10 min. The cells were incubated with ice-cold 70% ethanol on ice for more than 1 h or stored at −20°C overnight. For the cell cycle profile analysis, the cell pellets were incubated with 500 μl of PBS containing 10 μg/ml RNase (Sigma-Aldrich) and 20 μg/ml propidium iodide (PI, Sigma-Aldrich) at room temperature in the dark for 30 min, before subjecting them to a FACS analysis. For measuring the mitotic index, the cells were incubated with the anti-rabbit pH3-S10 (1:500, A301-844A, Bethyl) and then with the secondary antibody anti-rabbit IgG' fragment-Cy3 (1:200, C2306, Sigma-Aldrich). For the Annexin V staining, the cells including the medium were harvested and washed with PBS. The cell pellets were incubated with 1 μl of APC-Annexin V (BD Pharmingen™, Heidelberg, Germany) in 100 μl of the Annexin V binding buffer [10 mM HEPES/NaOH (pH 7.4), 140 mM NaCl, 2.5 mM $CaCl_2$] at room temperature in the dark for 15 min. About 400 μl of the Annexin V binding buffer containing 80 μg/ml DAPI was added, and the samples were analyzed by flow cytometry.

Live cell imaging

The cells were transfected with GFP-EV, GFP-MCPH1, or GFP-MCPH1-ΔDB2 into U2OS cells. After 24 h, the cells were recorded by live imaging using the microscope Olympus AX70 (Olympus, Tokyo, Japan) for 48 h.

In utero electroporation

An *in utero* electroporation was performed as described previously (Gruber *et al*, 2011). Briefly, 1 μm plasmid DNA in a TE buffer was injected into the lateral ventricle of E14.5 embryos followed by electroporation. The embryos were isolated 24 h (Cdh1 overexpression) or 48 h (for βTrCP2 overexpression) after electroporation and processed for cryosection and immunostaining.

Histological analysis

For the embryonic brains, the pregnant mice at the embryonic days E16.5 or E15.5 were sacrificed by cervical dislocation and the embryonic brains were isolated by decapitation and fixed overnight with 4% PFA at 4°C for 1–2 days. For the cryosections, tissues were cryoprotected in 30% sucrose at 4°C for 1–2 days, followed by freezing at −80°C. The cryoblocks were cut at 20 μm thickness by cryostate (Leica, Wetzlar, Germany), and the sections were stored at −80°C and processed for immunostaining.

Statistical analysis

The sampling distribution was tested using chi-squared test. Depending on the normality and variance equality, two-tailed Student's *t*-test was used. For samples containing multiple comparisons, one-way ANOVA test was used to measure statistical significance.

Expanded View for this article is available online.

Acknowledgements

We thank N. Andreas for his excellent assistance for the cytometry analysis. We also thank M. Rodriguez and P. Elsner for their excellent assistance in the maintenance of the animal colonies. We are also grateful to many other members of our laboratory for the helpful discussions. Further thank goes to E. Stoeckl for editing the manuscript. X.L. is supported by a fellowship from the Deutsche Forschungsgemeinschaft (DFG), supported by the Graduate School (RTG1715) and the Leibniz Graduate School of Ageing (LGSA) Program. This project is also supported by the DFG (to Z.-Q.W., WA2721/2-1), Germany.

Author contributions

XL conceived the project and performed the majority of the experiments. WZ participated in immunostaining and analysis staining cell lines and vector construction. TL helped vector construction. YW and XX performed yeast two-hybrid screening. Z-WZ performed living imaging and *in utero* electroporation.

© 2017 The Authors

XL, Z-WZ, and Z-QW designed the experiments and wrote the article. Z-QW supervised the project.

Conflict of interest

The authors declare that they have no conflict of interest.

References

Alderton GK, Galbiati L, Griffith E, Surinya KH, Neitzel H, Jackson AP, Jeggo PA, O'Driscoll M (2006) Regulation of mitotic entry by microcephalin and its overlap with ATR signalling. *Nat Cell Biol* 8: 725 – 733

Arai Y, Pulvers JN, Haffner C, Schilling B, Nusslein I, Calegari F, Huttner WB (2011) Neural stem and progenitor cells shorten S-phase on commitment to neuron production. *Nat Commun* 2: 154

Bassermann F, Frescas D, Guardavaccaro D, Busino L, Peschiaroli A, Pagano M (2008) The Cdc14B-Cdh1-Plk1 axis controls the G2 DNA-damage-response checkpoint. *Cell* 134: 256 – 267

Brown JA, Bourke E, Liptrot C, Dockery P, Morrison CG (2010) MCPH1/BRIT1 limits ionizing radiation-induced centrosome amplification. *Oncogene* 29: 5537 – 5544

Busino L, Donzelli M, Chiesa M, Guardavaccaro D, Ganoth D, Dorrello NV, Hershko A, Pagano M, Draetta GF (2003) Degradation of Cdc25A by beta-TrCP during S phase and in response to DNA damage. *Nature* 426: 87 – 91

Chavali PL, Putz M, Gergely F (2014) Small organelle, big responsibility: the role of centrosomes in development and disease. *Philos Trans R Soc Lond B Biol Sci* 369: 20130468

Cheffer A, Tarnok A, Ulrich H (2013) Cell cycle regulation during neurogenesis in the embryonic and adult brain. *Stem Cell Rev* 9: 794 – 805

Choudhury R, Bonacci T, Arceci A, Lahiri D, Mills CA, Kernan JL, Branigan TB, DeCaprio JA, Burke DJ, Emanuele MJ (2016) APC/C and SCF(cyclin F) constitute a reciprocal feedback circuit controlling S-phase entry. *Cell Rep* 16: 3359 – 3372

Delgado-Esteban M, Garcia-Higuera I, Maestre C, Moreno S, Almeida A (2013) APC/C-Cdh1 coordinates neurogenesis and cortical size during development. *Nat Commun* 4: 2879

Donzelli M, Squatrito M, Ganoth D, Hershko A, Pagano M, Draetta GF (2002) Dual mode of degradation of Cdc25 A phosphatase. *EMBO J* 21: 4875 – 4884

Fasanaro P, Capogrossi MC, Martelli F (2010) Regulation of the endothelial cell cycle by the ubiquitin-proteasome system. *Cardiovasc Res* 85: 272 – 280

Gavvovidis I, Rost I, Trimborn M, Kaiser FJ, Purps J, Wiek C, Hanenberg H, Neitzel H, Schindler D (2012) A novel MCPH1 isoform complements the defective chromosome condensation of human MCPH1-deficient cells. *PLoS One* 7: e40387

Gruber R, Zhou Z, Sukchev M, Joerss T, Frappart PO, Wang ZQ (2011) MCPH1 regulates the neuroprogenitor division mode by coupling the centrosomal cycle with mitotic entry through the Chk1-Cdc25 pathway. *Nat Cell Biol* 13: 1325 – 1334

Hainline SG, Rickmyre JL, Neitzel LR, Lee LA, Lee E (2014) The *Drosophila* MCPH1-B isoform is a substrate of the APCCdh1 E3 ubiquitin ligase complex. *Biol Open* 3: 669 – 676

Hemelaar J, Borodovsky A, Kessler BM, Reverter D, Cook J, Kolli N, Gan-Erdene T, Wilkinson KD, Gill G, Lima CD, Ploegh HL, Ovaa H (2004) Specific and covalent targeting of conjugating and deconjugating enzymes of ubiquitin-like proteins. *Mol Cell Biol* 24: 84 – 95

Hershko A, Ciechanover A (1998) The ubiquitin system. *Annu Rev Biochem* 67: 425 – 479

Hussain MS, Baig SM, Neumann S, Peche VS, Szczepanski S, Nurnberg G, Tariq M, Jameel M, Khan TN, Fatima A, Malik NA, Ahmad I, Altmuller J, Frommolt P, Thiele H, Hohne W, Yigit G, Wollnik B, Neubauer BA, Nurnberg P *et al* (2013) CDK6 associates with the centrosome during mitosis and is mutated in a large Pakistani family with primary microcephaly. *Hum Mol Genet* 22: 5199 – 5214

Jackson AP, Eastwood H, Bell SM, Adu J, Toomes C, Carr IM, Roberts E, Hampshire DJ, Crow YJ, Mighell AJ, Karbani G, Jafri H, Rashid Y, Mueller RF, Markham AF, Woods CG (2002) Identification of microcephalin, a protein implicated in determining the size of the human brain. *Am J Hum Genet* 71: 136 – 142

Jeffers LJ, Coull BJ, Stack SJ, Morrison CG (2008) Distinct BRCT domains in Mcph1/Brit1 mediate ionizing radiation-induced focus formation and centrosomal localization. *Oncogene* 27: 139 – 144

Jin J, Shirogane T, Xu L, Nalepa G, Qin J, Elledge SJ, Harper JW (2003) SCFbeta-TRCP links Chk1 signaling to degradation of the Cdc25A protein phosphatase. *Genes Dev* 17: 3062 – 3074

Kaindl AM (2014) Autosomal recessive primary microcephalies (MCPH). *Eur J Paediatr Neurol* 18: 547 – 548

Kuipers MA, Stasevich TJ, Sasaki T, Wilson KA, Hazelwood KL, McNally JG, Davidson MW, Gilbert DM (2011) Highly stable loading of Mcm proteins onto chromatin in living cells requires replication to unload. *J Cell Biol* 192: 29 – 41

van Leuken R, Clijsters L, Wolthuis R (2008) To cell cycle, swing the APC/C. *Biochim Biophys Acta* 1786: 49 – 59

Lin SY, Rai R, Li K, Xu ZX, Elledge SJ (2005) BRIT1/MCPH1 is a DNA damage responsive protein that regulates the Brca1-Chk1 pathway, implicating checkpoint dysfunction in microcephaly. *Proc Natl Acad Sci USA* 102: 15105 – 15109

Lin SY, Liang Y, Li K (2010) Multiple roles of BRIT1/MCPH1 in DNA damage response, DNA repair, and cancer suppression. *Yonsei Med J* 51: 295 – 301

Mai L, Yi F, Gou X, Zhang J, Wang C, Liu G, Bu Y, Yuan C, Deng L, Song F (2014) The overexpression of MCPH1 inhibits cell growth through regulating cell cycle-related proteins and activating cytochrome c-caspase 3 signaling in cervical cancer. *Mol Cell Biochem* 392: 95 – 107

Margottin-Goguet F, Hsu JY, Loktev A, Hsieh HM, Reimann JD, Jackson PK (2003) Prophase destruction of Emi1 by the SCF(betaTrCP/Slimb) ubiquitin ligase activates the anaphase promoting complex to allow progression beyond prometaphase. *Dev Cell* 4: 813 – 826

Matsuda T, Cepko CL (2004) Electroporation and RNA interference in the rodent retina *in vivo* and *in vitro*. *Proc Natl Acad Sci USA* 101: 16 – 22

Meghini F, Martins T, Tait X, Fujimitsu K, Yamano H, Glover DM, Kimata Y (2016) Targeting of Fzr/Cdh1 for timely activation of the APC/C at the centrosome during mitotic exit. *Nat Commun* 7: 12607

Mirzaa GM, Vitre B, Carpenter G, Abramowicz I, Gleeson JG, Paciorkowski AR, Cleveland DW, Dobyns WB, O'Driscoll M (2014) Mutations in CENPE define a novel kinetochore-centromeric mechanism for microcephalic primordial dwarfism. *Hum Genet* 133: 1023 – 1039

Neitzel H, Neumann LM, Schindler D, Wirges A, Tonnies H, Trimborn M, Krebsova A, Richter R, Sperling K (2002) Premature chromosome condensation in humans associated with microcephaly and mental retardation: a novel autosomal recessive condition. *Am J Hum Genet* 70: 1015 – 1022

Peng G, Yim EK, Dai H, Jackson AP, Burgt I, Pan MR, Hu R, Li K, Lin SY (2009) BRIT1/MCPH1 links chromatin remodelling to DNA damage response. *Nat Cell Biol* 11: 865 – 872

 © 2017 The Authors

Rai R, Dai H, Multani AS, Li K, Chin K, Gray J, Lahad JP, Liang J, Mills GB, Meric-Bernstam F, Lin SY (2006) BRIT1 regulates early DNA damage response, chromosomal integrity, and cancer. *Cancer Cell* 10: 145 – 157

Roberts E, Hampshire DJ, Pattison L, Springell K, Jafri H, Corry P, Mannon J, Rashid Y, Crow Y, Bond J, Woods CG (2002) Autosomal recessive primary microcephaly: an analysis of locus heterogeneity and phenotypic variation. *J Med Genet* 39: 718 – 721

Singh N, Wiltshire TD, Thompson JR, Mer G, Couch FJ (2012) Molecular basis for the association of microcephalin (MCPH1) protein with the cell division cycle protein 27 (Cdc27) subunit of the anaphase-promoting complex. *J Biol Chem* 287: 2854 – 2862

Suzuki H, Chiba T, Kobayashi M, Takeuchi M, Suzuki T, Ichiyama A, Ikenoue T, Omata M, Furuichi K, Tanaka K (1999) IkappaBalpha ubiquitination is catalyzed by an SCF-like complex containing Skp1, cullin-1, and two F-box/WD40-repeat proteins, betaTrCP1 and betaTrCP2. *Biochem Biophys Res Commun* 256: 127 – 132

Suzuki H, Chiba T, Suzuki T, Fujita T, Ikenoue T, Omata M, Furuichi K, Shikama H, Tanaka K (2000) Homodimer of two F-box proteins betaTrCP1 or betaTrCP2 binds to IkappaBalpha for signal-dependent ubiquitination. *J Biol Chem* 275: 2877 – 2884

Tang X, Orlicky S, Lin Z, Willems A, Neculai D, Ceccarelli D, Mercurio F, Shilton BH, Sicheri F, Tyers M (2007) Suprafacial orientation of the SCFCdc4 dimer accommodates multiple geometries for substrate ubiquitination. *Cell* 129: 1165 – 1176

Tapias A, Zhou ZW, Shi Y, Chong Z, Wang P, Groth M, Platzer M, Huttner W, Herceg Z, Yang YG, Wang ZQ (2014) Trrap-dependent histone acetylation specifically regulates cell-cycle gene transcription to control neural progenitor fate decisions. *Cell Stem Cell* 14: 632 – 643

Thomas Y, Coux O, Baldin V (2010) betaTrCP-dependent degradation of CDC25B phosphatase at the metaphase-anaphase transition is a pre-requisite for correct mitotic exit. *Cell Cycle* 9: 4338 – 4350

Trimborn M, Bell SM, Felix C, Rashid Y, Jafri H, Griffiths PD, Neumann LM, Krebs A, Reis A, Sperling K, Neitzel H, Jackson AP (2004) Mutations in microcephalin cause aberrant regulation of chromosome condensation. *Am J Hum Genet* 75: 261 – 266

Trimborn M, Schindler D, Neitzel H, Hirano T (2006) Misregulated chromosome condensation in MCPH1 primary microcephaly is mediated by condensin II. *Cell Cycle* 5: 322 – 326

Vodermaier HC (2004) APC/C and SCF: controlling each other and the cell cycle. *Curr Biol* 14: R787 – R796

Weischenfeldt J, Damgaard I, Bryder D, Theilgaard-Monch K, Thoren LA, Nielsen FC, Jacobsen SE, Nerlov C, Porse BT (2008) NMD is essential for hematopoietic stem and progenitor cells and for eliminating by-products of programmed DNA rearrangements. *Genes Dev* 22: 1381 – 1396

Welcker M, Clurman BE (2008) FBW7 ubiquitin ligase: a tumour suppressor at the crossroads of cell division, growth and differentiation. *Nat Rev Cancer* 8: 83 – 93

Wood JL, Liang Y, Li K, Chen J (2008) Microcephalin/MCPH1 associates with the Condensin II complex to function in homologous recombination repair. *J Biol Chem* 283: 29586 – 29592

Xu X, Lee J, Stern DF (2004) Microcephalin is a DNA damage response protein involved in regulation of CHK1 and BRCA1. *J Biol Chem* 279: 34091 – 34094

Yamashita Y, Kasugai I, Sato M, Tanuma N, Sato I, Nomura M, Yamashita K, Sonoda Y, Kumabe T, Tominaga T, Katakura R, Shima H (2010) CDC25A mRNA levels significantly correlate with Ki-67 expression in human glioma samples. *J Neurooncol* 100: 43 – 49

Yang SZ, Lin FT, Lin WC (2008) MCPH1/BRIT1 cooperates with E2F1 in the activation of checkpoint, DNA repair and apoptosis. *EMBO Rep* 9: 907 – 915

Young LM, Pagano M (2010) Cdc25 phosphatases: differential regulation by ubiquitin-mediated proteolysis. *Cell Cycle* 9: 4613 – 4614

Yu X, Chini CC, He M, Mer G, Chen J (2003) The BRCT domain is a phospho-protein binding domain. *Science* 302: 639 – 642

Zhou Z, Sun X, Zou Z, Sun L, Zhang T, Guo S, Wen Y, Liu L, Wang Y, Qin J, Li L, Gong W, Bao S (2010) PRMT5 regulates Golgi apparatus structure through methylation of the golgin GM130. *Cell Res* 20: 1023 – 1033

Zhou ZW, Tapias A, Bruhn C, Gruber R, Sukchev M, Wang ZQ (2013) DNA damage response in microcephaly development of MCPH1 mouse model. *DNA Repair (Amst)* 12: 645 – 655

Zhou L, Bai Y, Li Y, Liu X, Tan T, Meng S, He W, Wu X, Dong Z (2016) Overexpression of MCPH1 inhibits uncontrolled cell growth by promoting cell apoptosis and arresting the cell cycle in S and G2/M phase in lung cancer cells. *Oncol Lett* 11: 365 – 372

© 2017 The Authors